

Handcrafted and Deep Trackers: A Review of Recent Object Tracking Approaches

Mustansar Fiaz, Arif Mahmood , Sajid Javed and Soon Ki Jung

In recent years visual object tracking has become a very active research area. An increasing number of tracking algorithms are being proposed each year. It is because tracking has wide applications in various real world problems such as human-computer interaction, autonomous vehicles, robotics, surveillance and security just to name a few. In the current study, we review latest trends and advances in the tracking area and evaluate the robustness of different trackers based on the feature extraction methods. The first part of this work comprises a comprehensive survey of the recently proposed trackers. We broadly categorize trackers into Correlation Filter based Trackers (CFTs) and Non-CFTs. Each category is further classified into various types based on the architecture and the tracking mechanism. In the second part, we experimentally evaluated 24 recent trackers for robustness, and compared handcrafted and deep feature based trackers. We observe that trackers using deep features performed better, though in some cases a fusion of both increased performance significantly. In order to overcome the drawbacks of the existing benchmarks, a new benchmark Object Tracking and Temple Color (OTTC) has also been proposed and used in the evaluation of different algorithms. We analyze the performance of trackers over eleven different challenges in OTTC, and three other benchmarks. Our study concludes that Discriminative Correlation Filter (DCF) based trackers perform better than the others. Our study also reveals that inclusion of different types of regularizations over DCF often results in boosted tracking performance. Finally, we sum up our study by pointing out some insights and indicating future trends in visual object tracking field.

Index Terms—Visual Object Tracking; Robustness of Tracking Algorithms, Surveillance, Tracking Evaluation.

I. INTRODUCTION

Visual Object Tracking (VOT) is a promising but difficult sub-field of computer vision. It attained much reputation because of its widespread use in different applications for instance autonomous vehicles [1], traffic flow monitoring [2], surveillance and security [3], human machine interaction [4], medical diagnostic systems [5], and activity recognition [6]. VOT is an attractive research area of computer vision due to opportunities and different tracking challenges. In the previous few decades, remarkable endeavors are made by research community, but still VOT has much potential to explore further. The difficulty of VOT lies in the myriad of challenges, such as occlusion, background clutter, illumination changes, scale variation, low resolution, fast motion, out of view, motion blur, deformation, in and out planer rotation [7], [8].

VOT is the process of identifying a region of interest in a sequence and consists of four sequential elements, including target initialization, appearance model, motion prediction, and target positioning. Target initialization is the process of annotating object position, or region of interest, with any of the following representations: object bounding box, ellipse, centroid, object skeleton, object contour, or object silhouette. Usually, an object bounding box is provided in the initial frame of a sequence and the tracking algorithm estimates target position in the remaining frames. Appearance modelling

Mustansar Fiaz, School of Computer Science and Engineering, Kyungpook National University, Deagu, Republic of Korea, Email: mustansar@vr.knu.ac.kr

Arif Mahmood, Department of Computer Science, Information Technology University, Lahore, Pakistan Email: arif.mahmood@itu.edu.pk

Sajid Javed, Department of Computer Science, Tissue Image Analytics Laboratory, University of Warwick, United Kingdom, Email: s.javed.1@warwick.ac.uk

Soon Ki Jung, School of Computer Science and Engineering, Kyungpook National University, Deagu, Republic of Korea, Corresponding author email: skjung@knu.ac.kr

is composed of identifying visual object features for better representation of a region of interest and effective construction of mathematical models to detect objects using learning techniques. In motion prediction, the target location is estimated in subsequent frames. The target positioning operation involves maximum posterior prediction, or greedy search. Tracking problems can be simplified by constraints imposed on the appearance and motion models. During the tracking, new target appearance is integrated by updating the appearance and motion models.

Currently, we have focused on monocular, model-free, single-target, causal, and short-term trackers for experimental study. The *model-free* characteristics hold for supervised training example in the initial frame provided by bounding box. The *causality* means that tracker will predict the target location on current frame without prior knowledge of future frames. While, *short-term* means that if a tracker is lost (fails) during the tracking, re-detection is not possible. And trackers output is specified by a bounding box.

Literature shows that much research has been performed on object tracking and various surveys have been published. An excellent and extensive review of tracking algorithms is presented in [9] along with feature representations and challenges. However, the field has greatly advanced in recent years. Cannons et al. [10] covered the fundamentals of object tracking problems, and discussed the building blocks for object tracking algorithms, the evolution of feature representations and different tracking evaluation techniques. Smeulders et al. [11] compared the performance of tracking algorithms and introduced a new benchmark. Li et al. [12] and Yang et al. [13] discussed object appearance representations, and performed surveys for online generative and discriminative learning. Most of the surveys are somewhat outdated and subject to traditional tracking methods. Recently, the performance of tracking algorithm was boosted by the inclusion of deep

learning techniques. Li et. al [14] classified the deep trackers into Network Structure (NS), Network Function (NF), and Network Training (NT). Moreover, VOT challenge [15], [16], [17], [18], [19] is providing the efficient comparison of the various trackers based and their brief introduction. However, our study differs in terms of organizing tracking schemes based on their tracking framework. Our study differs in two aspects: (1) recent tracking approaches and (2) Comparative study of trackers based on their feature extraction method.

The objective of the current study is to provide an overview of the recent progress, research trends, and to categorize existing tracking algorithms. Our motivation is to provide interested readers an organized reference about the diverse tracking algorithms being developed, to help them find research gaps, and provide insights for developing new tracking algorithms.

Features play an important role in the performance of a tracker. There are two broad categories of the features used by the tracking algorithms including HandCrafted (HC) and deep features. HC features such as Histogram of Oriented Gradients (HOG), Scale-Invariant Feature Transform (SIFT), Local Binary Pattern (LBP) and color names were commonly used to represent target appearance. Recently researchers have shifted their methodology and focus deep features. Deep learning has shown remarkable success in various computer vision tasks such as object recognition and tracking, image segmentation, pose estimation, and image captioning. Deep features have many advantages over HC features because of having more potential to encode multi-level information and exhibit more invariance to target appearance variations. There are various deep feature extraction methods including Recurrent Neural Networks (RNN) [20], Convolutional Neural Networks (CNN) [21], Residual Networks [22], and Auto-encoders [23]. In contrast to HC approaches, deep models are data-hungry and requiring a lot of training data. In applications with scarce training data, deep features are extracted using off-the-shelf pre-trained models such as VGGNet [21]. Despite the fact that deep features have achieved much success in single object tracking [24], [25], [26] but still HC features [27], [28] produce comparative results and are being employed in tracking algorithms. We have investigated different trackers performance on the basis of HC, deep features and combination of these features to get the broader aspect of the role of features in tracking performance.

As mentioned earlier, visual object tracking faces several challenges and therefore numerous algorithms are introduced. For example Zhang et al. [29], Pan and Hu [30] and Yilmaz et al. [31] proposed tracking algorithms to handle occlusion in videos. Similarly, to handle illumination variations, algorithms have been proposed by Zhang et al. [32], Adam et al. [33], and Babenko et al. [34]. Moreover, Mei et al. [35], Kalal et al. [36], and Kwon et al. [37] handled the problem of cluttered background. Likewise, various tracking techniques have been developed to deal with other tracking challenges. Hence, there is a dire need to organize the literature associated with these challenges, to analyze the robustness of the trackers, and to categorize these algorithms according to the challenges available in the existing benchmarks. In the current work, we categorized the trackers according to feature representation

schemes such as handcrafted and deep feature based trackers, and analyzed the performance over eleven different challenges.

The rest of this paper is organized as follows: Section II demonstrates related work; the classification of recent tracking algorithms and their brief introduction is explained in section III; experimental investigation is described in section IV; and the conclusion and future directions are described in section V.

II. RELATED WORK

The research community has shown keen interest in VOT, and developed various state-of-the-art tracking algorithms. Therefore, an overview of research methodologies and techniques will be helpful in organizing domain knowledge. Trackers can be categorized as single-object vs. multiple-object trackers, generative vs. discriminative, context-aware vs. non-aware, and online vs. offline learning algorithms. Single object trackers [38], [39] are the algorithms tracking only one object in the sequence, while multi-object trackers [40], [41] simultaneously track multiple targets and follow their trajectories. In generative models, the tracking task is carried out via searching the best-matched window, while discriminative models discriminate target patch from the background [42], [43], [13]. In the current paper, recent tracking algorithms are classified as Correlation-Filter based Trackers (CFTs) and Non-CFTs (NCFTs). It is obvious from the names that CFTs [44], [45], [46] utilize correlation filters, and non-correlation trackers use other techniques [47], [48], [49].

Yilmaz et al. [9] presented a taxonomy of tracking algorithms and discussed tracking methodologies, feature representations, data association, and various challenges. Yang et al. [13] presented an overview of the local and global feature descriptors used to present object appearance, and reviewed on-line learning techniques such as generative versus discriminative, Monte Carlo sampling techniques, and integration of contextual information for tracking. Cannons [10] discussed object tracking components initialization, representations, adaption, association and estimation. He discussed the advantages and disadvantages of different feature representations and their combinations. Smeulders et al. [11] performed analysis and evaluation of different trackers with respect to a variety of tracking challenges. They found sparse and local features more suited to handle illumination variations, background clutter, and occlusion. They used various evaluation techniques, such as survival curves, Grubbs testing, and Kaplan Meier statistics, and provided evidence that F-score is the best measure of tracking performance. Li et al. [12] gave a detailed summary of target appearance models. Their study included local and global feature representations, discriminative, and generative, and hybrid learning techniques. In recent times, deep learning has shown significant progress in visual trackers and Li et al. [14] categorized deep learning trackers into three aspects: (1) network structure; network function; and network training.

Some relatively limited or focused reviews include the following works. Qi et al. [50] focused on classification of online single target trackers. Zhang et al. [51] discussed tracking based on sparse coding, and classified sparse trackers. Ali et al.

[3] discussed some classical tracking algorithms. Yang et al. [52] considered context of tracking scene considering auxiliary objects [53] as the target context. Chen et al. [54] examined only CFTs. Arulampalam et al. [55] presented Bayesian tracking methods using particle filters. Most of these studies are outdated or consider only few algorithms and thus are limited in scope. In contrast, we presented a more comprehensive survey of recent contributions. We classified tracking algorithms as CFTs and NCFTs. We evaluated the performance accuracy of HC and deep trackers. Moreover, tracking robustness has been examined over different challenges.

III. CLASSIFICATION OF TRACKING ALGORITHMS

In this section, recent tracking algorithms are studied and most of them are proposed during the last four years. Each algorithm presents a different method to exploit target structure for predicting target location in a sequence. By analyzing the tracking procedure, we arrange these algorithms in a hierarchy and classify them into two main categories: Correlation Filter Trackers (CFT) and Non-CFT (NCFT) with a number of subcategories in each class.

A. Correlation Filter Trackers

Discriminative Correlation Filters (DCF) are actively utilized in various computer vision applications including object recognition [56], image registration [57], face verification [58], and action recognition [59]. In object tracking, Correlation Filters (CF) have been used to improve robustness and efficiency. Initially, the requirement of training made CF inappropriate for online tracking. In the later years, the development of Minimum Output of Sum of Squared Error (MOSSE) filter [60], that allows for efficient adaptive training, changed the situation. The objective of the MOSSE filter is to minimize the sum of the squared error between the desired output and actual output in Fourier domain. MOSSE is an improved version of Average Synthetic Exact Filter (ASEF) [61] which is trained offline to detect objects. ASEF computes mean for a set of exact filters, each computed from a different training image of the same object, to get best filter at the output. Later on, many state-of-the-art CFT were proposed based on MOSSE. Traditionally, the aim of designing inference of CF is to yield response map that has low value for background and high value for region of interest in the scene. One such algorithm is Circulant Structure with Kernel (CSK) tracker [62], which exploits circulant structure of the target appearance and is trained using kernel regularized least squares method.

CF-based tracking schemes perform computation in the frequency domain to manage computational cost. General architecture of these algorithms follow "tracking-by-detection" approach and is presented in Fig. 2. Correlation filters are initialized from the initial frame of the sequence with a target patch cropped at the target position. During tracking, the target location is estimated in the new upcoming frame using the target estimated position in the last frame. To effectively represent appearance of the target, appropriate feature extraction method is employed to construct feature map from the input patch. Boundaries are smoothed by applying a cosine

filter. Correlation operation is performed instead of exhausted convolution operation. The response map is computed using Element-wise multiplication between adaptive learning filter and extracted features, and by using a Discrete Fourier Transform (DFT). DFT operates in the frequency domain using Fast Fourier Transform (FFT). Confidence map is obtained in spatial domain by applying Inverse FFT (IFFT) over the response map. The maximum confidence score estimates the new target position. At the outcome, the target appearance at the newly predicted location is updated by extracting features and updating correlation filters.

Let h be a correlation filter and x be the current frame, which may consist of the extracted features or the raw image pixels. CNN convolutional filters perform similar to correlation filters in Fourier domain. According to convolution theorem, correlation in frequency domain that computes a response map by performing element-wise multiplication between zero padded versions of $f(h)$ and $f(x)$ is equivalent to circulant convolution in spatial domain. Often h is of much smaller size compared to x , therefore before transformation to Fourier domain, zero padding is used such that transformed sizes of both are the same.

$$x \otimes h = \mathfrak{F}^{-1}(\hat{x} \odot \hat{h}^*), \quad (1)$$

where \mathfrak{F}^{-1} indicates the IFFT, $\hat{\cdot}$ denotes Fourier representation, \otimes represents convolution, \odot means element-wise multiplication, and $*$ is the complex conjugate. Equation yields a confidence map between x and h . To update the correlation filter, the estimated target around the maximum confidence position is selected. Assume y is the desired output. Correlation filter h must satisfy for new target appearance z as:

$$y = \mathfrak{F}^{-1}(\hat{z} \odot \hat{h}^*), \quad \hat{h}^* = \hat{y}/\hat{z}, \quad (2)$$

where \hat{y} denotes the desired output y in frequency domain and division operation is performed during element-wise multiplication. FFT reduces the computational cost, as circulant convolution has a complexity of $O(n^4)$ for image size $n \times n$ while FFT require only $O(n^2 \log n)$.

CF-based tracking frameworks face different difficulties, such as the training of the target appearance (orientation, and shape), as it may change over time. Another challenge is the selection of an efficient feature representation, as powerful features may improve the performance of CFTs. Another important challenge for CFTs is scale adaption, as the size of correlation filters are fixed during tracking. A target may change its scale over time. Furthermore, if the target is lost then it cannot be recovered again. CFTs are further divided into the categories *B*-CFTs, regularized CFTs, part-based, Siamese-based, and Fusion-based CFTs as explained below.

1) Basic Correlation Filter based Trackers

Basic-CFTs are tackers that use Kernelized Correlation Filters (KCF) [63] as their baseline tracker. Trackers may use different features such as the HOG, colour names (CN) [64] and deep features using Recurrent Neural Networks (RNN) [65], Convolutional Neural Networks (CNN) [21], and Residual Networks [22]. Numerous trackers have been developed using KCF as base tracker including [66], [67], [68], [69],

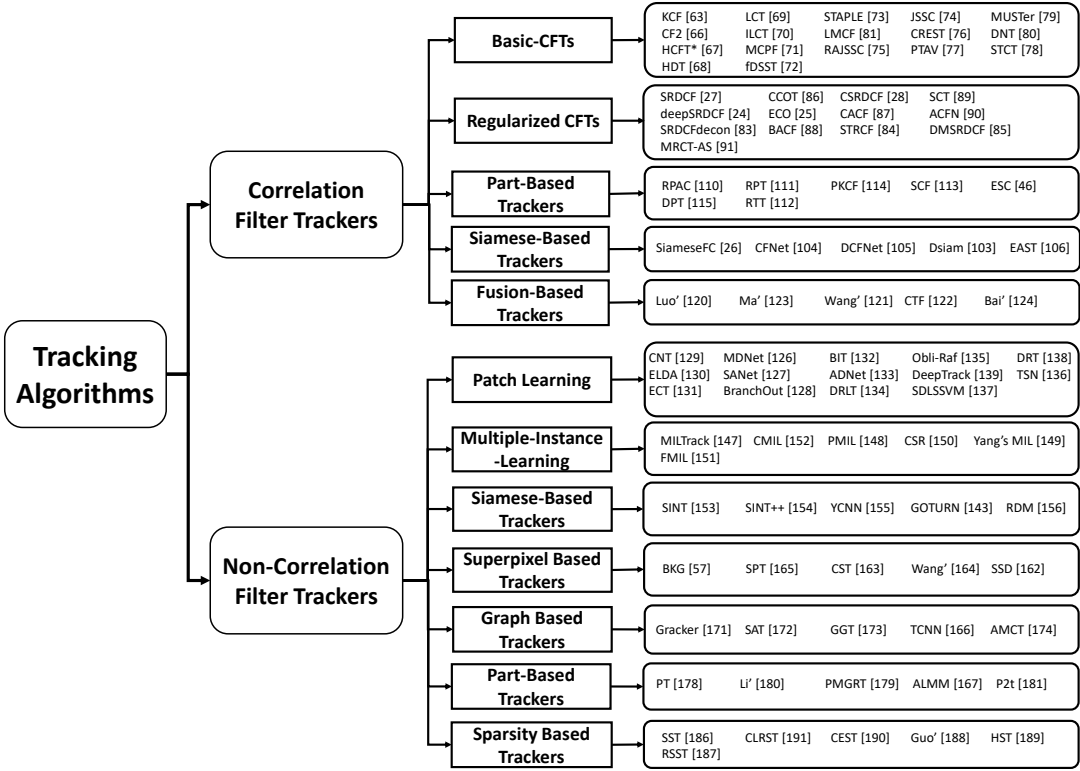


Fig. 1. Taxonomy of tracking algorithms.

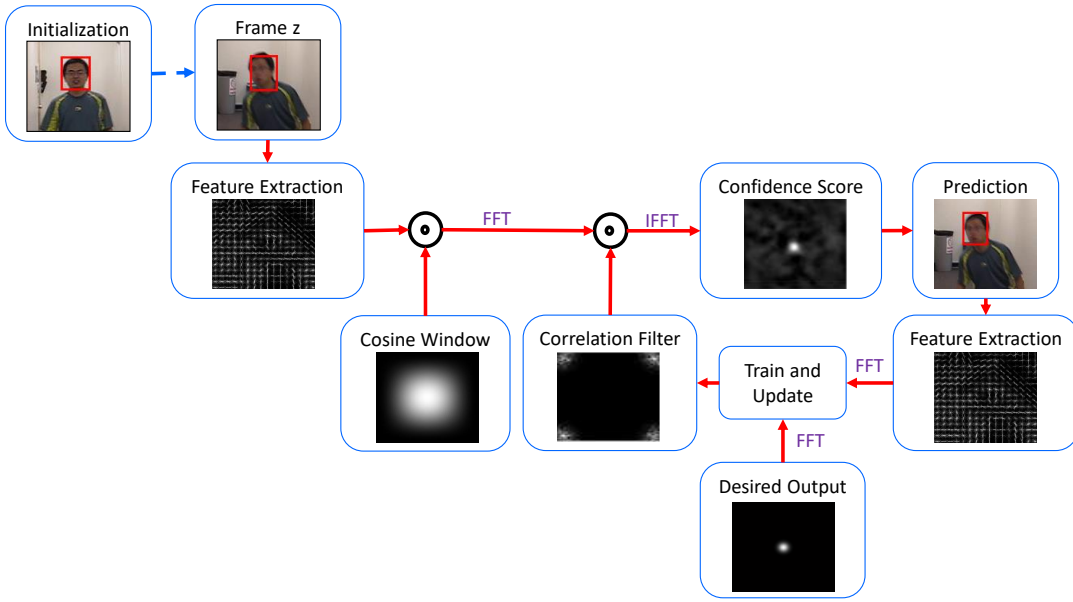


Fig. 2. The framework of correlation filter for visual object tracking [54].

[70], [71], [72], [73], [74], [75], [76], [77], [78], [79], [80], [81].

A KCF [63] algorithm performs tracking using Gaussian kernel function for distinguishing between target object and its surroundings. HOG descriptors of cell size four is employed by KCF. During tracking, an image patch is cropped in new frame, HOG features are computed for that patch, and a response map is computed by multiplying adaptive filters on input features in Fourier domain. A new target position is predicted at the position of maximum confidence score in the confidence map obtained by applying inverse Fourier transform on response map. A new patch containing object is then cropped and HOG features are recomputed to update the CF.

Ma et al.[66] exploited rich hierarchical Convolutional Features using CF represented as CF2 (Fig. 3). For every subsequent frame, the search area is cropped at the center based on previously predicted target position. Three hierarchical convolutional features are extracted from VGGNet layers conv3-4, conv4-4, and conv5-4 to exploit target appearance. Deep features are resized to the same size using bilinear interpolation. An independent adaptive CF is utilized for each CNN feature, and response maps are computed. A coarse-to-fine methodology is applied over the set of correlation response maps to estimate the new target position. Adaptive hierarchical CFs are updated on newly-predicted target location. Ma et al. [67] also proposed Hierarchical Correlation Feature based Tracker (HCFT*), which is an extension of CF2 that integrates re-detection and scale estimation of target.

The Hedged Deep Tracking (HDT) [68] algorithm takes advantage of multiple levels of CNN features. In HDT, authors hedged many weak trackers together to attain a single strong tracker. During tracking, the target position at the previous frame is utilized to crop a new image to compute six deep features using VGGNet. Deep features are exploited to individual CF to compute response maps also known as weak experts. The target position is estimated by each weak tracker, and the loss for each expert is also computed. A standard hedge algorithm is used to estimate the final position. All weak trackers are hedged together into a strong single tracker by applying an adaptive online decision algorithm. Weights for each weak tracker are updated during online tracking. In an adaptive Hedge algorithm, a regret measure is computed for all weak trackers as a weighted average loss. A stability measure is computed for each expert based on the regret measure. The hedge algorithm strives to minimize the cumulative regret of weak trackers depending upon its historical information.

The Long-term Correlation Tracking (LCT) [69] involves exclusive prediction of target translation and scale using correlation filters and random fern classifier [82] is used for online re-detection of the target during tracking. In LCT algorithms, the search window is cropped on the previously estimated target location and a feature map is computed. Translation estimation is performed using adaptive translation correlation filters. A target pyramid is generated at the newly predicted target translation position, and scale is estimated using a separate regression correlation model. In case of failure, the LCT tracking algorithm performs re-detection. If

the estimated target score is less then a threshold, re-detection is then performed using online random fern classifier. Average response is computed using posteriors from all the ferns. LCT selects the positive samples to predict new patch as target by using the k -nearest neighbor (KNN) classifier. Author has further Improved LCT (ILCT) [70] using SVM classifier instead of fern classifier for re-detection.

The Multi-task Correlation Particle Filter (MCPF) proposed by Zhang et al. [71] employ particle filter framework. The MCPF shepherd particles in the search region by exploiting all states of the target. The MCPF computes response maps of particles, and target position is estimated as weighted sum of the response maps. Danelljan et al. [72] proposed Discriminative Scale Space Tracking (DSST) to separately estimate translation and scale by learning independent CFs. Scale estimation is done by learning the target sample at various scale variations. In proposed framework, first translation is predicted by applying a standard translation filter to every incoming frame. After translation estimation, the target size is approximated by employing trained scale filter at the target location obtained by the translation filter. This way, the proposed strategy learns the target appearance induced by scale rather than by using exhaustive target size search methodologies. The author further improved the computational performance without sacrificing the robustness and accuracy. Fast DSST (fDSST) employs sub-grid interpolation to compute correlation scores.

The Sum of Template And Pixel-wise LEarners (STAPLE) [73] employed two separate regression models to solve the tracking problem by utilizing the inherent structure for each target representation. The tracking design takes advantage of two complementary factors from two different patch illustrations to train a model. HOG features and global color histograms are used to represent the target. In the colour template, foreground and background regions are computed at previously estimated location. The frequency of each colour bin for object and background are updated, and a regression model for colour template is computed. In the search area, a per-pixel score is calculated based on previously estimated location, and the integral image is used to compute response, while for the HOG template, HOG features are extracted at the position predicted in the previous frame, and CF are updated. At every incoming frame, a search region is extracted centered at previous estimated location, and their HOG features are convolved with CF to obtain a dense template response. Target position is estimated from template and histogram response scores as a linear combination. Final estimated location is influenced by the model which has more scores.

The Convolutional RESidual learning for visual Tracking (CREST) algorithm [76] utilizes residual learning [22] to adapt target appearance and also performs scale estimation by searching patches at different scales. During tracking, the search patch is cropped at previous location, and convolutional features are computed. Residual and base mapping are used to compute the response map. The maximum response value gives the newly estimated target position. Scale is estimated by exploring different scale patches at newly estimated target center position. The Parallel Tracking And Verifying (PTAV)

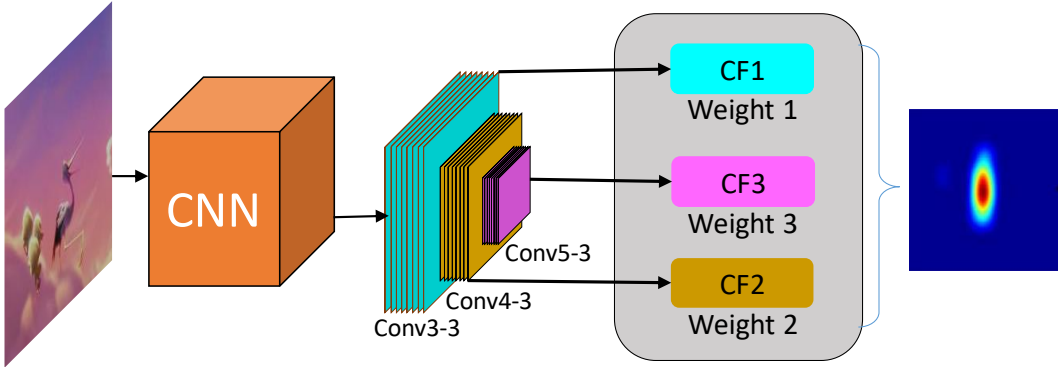


Fig. 3. CF2 framework [66].

[77] is composed of two major modules, i.e. tracker and verifier. Tracker module is responsible for computing the real time inference and estimate tracking results, while the verifier is responsible for checking whether the results are correct or not. The Multi-Store tracker (MUSTer) [79] avoid drifting and stabilizes the tracking by aggregating image information using short and long term stores, and is based on the Atkinson-Shiffrin memory model. Short term storage involves an integrated correlation filter to incorporate spatiotemporal consistency, while long term storage involves integrated RANSAC estimation and key point match tracking to control the output.

2) Regularized Correlation Filter Trackers

Discriminative CF (DCF) tracking algorithms are limited in their detection range because they require filter size and patch size to be equal. The DCF may learn the background for irregularly-shaped target objects. The DCF is formulated from periodic assumption, learns from a set of training samples, and thus may learn negative training patches. DCF response maps have accurate scores close to the centre, while other scores are influenced due to periodic assumption, thus degrading DCF performance. Another limitation of DCFs is that they are restricted to only a fixed search region. DCF trackers perform poorly on a target deformation problem due to over fitting of model caused by learning from target training samples but missing the negative samples. Thus, the tracker fails to re-detect in case of occlusion. A larger search region may solve the occlusion problem but the model will learn background information which degrades the discrimination power of the tracker. Therefore, there is a need to incorporate a measure of regularization for these DCF limitations and those trackers are classified as **Regularized Correlation Filter Trackers** (R-CFTs). Several R-CFTs have been proposed such as [27], [24], [83], [84], [85], [86], [25], [28], [87], [88], [89], [90], [91].

Danelljan et al.[27] presented Spatially Regularized DCF (SRDCF) by introducing spatial regularization in DCF learning. During tracking, the regularization component weakens the background information as shown in Fig. 4. Spatial regularization constraints the filter coefficients based on spatial information. The background is suppressed by assigning higher values to the coefficients that are located outside the target territory and vice versa. The SRDCF framework has

been updated by using deep CNN features in deepSRDCF [24]. The SRDCF framework has also been modified to handle contaminated training samples in SRDCFdecon [83]. It down weights corrupted training samples and estimate good quality samples. SRDCFdecon extracts training samples from previous frames and then assign higher weights to correct training patches. SRDCFdecon performs joint adaptation of both appearance model and weights of the training samples.

Li et al. [84] introduced the temporal regularization in SRDCF and introduced Spatial-Temporal Regularized CF (STRCF). Temporal regularization has been induced using passive aggressive learning to SRDCF with single image. Recently, deep motion features have been used for activity recognition [92]. Motion features are obtained from information obtained directly from optical flow applied to images. A CNN is then applied to optical flow to get deep motion features. Gladh et al.[85] presented Deep Motion SRDCF (DMSRDCF) which fused deep motion features along with hand-crafted appearance features using SRDCF as baseline tracker. Motion features are computed as reported by [93]. Optical flow is calculated on each frame on previous frame. The x, y components and magnitude of optical flow constitute three channels in the flow map, which is normalized between 0 and 255 and fed to the CNN to compute deep motion features.

Danelljan et al.[86] proposed learning multi-resolution feature maps, which they name as Continuous Convolutional Operators for Tracking (CCOT). The convolutional filters are learned in a continuous sequence of resolutions which generates a sequence of response maps. These multiple response maps are then fused to obtain final unified response map to estimate target position. The Efficient Convolution Operators (ECO) [25] tracking scheme is an improved version of CCOT. The CCOT learns a large number of filters to capture target representation from high dimensional features, and updates the filter for every frame, which involves training on a large number of sample sets. In contrast, ECO constructs a smaller set of filters to efficiently capture target representation using matrix factorization. The CCOT learns over consecutive samples in a sequence which forgets target appearance for a long period thus causes overfitting to the most recent appearances and leading to high computational cost. In contrast, ECO uses a Gaussian Mixture Model (GMM) to represent diverse

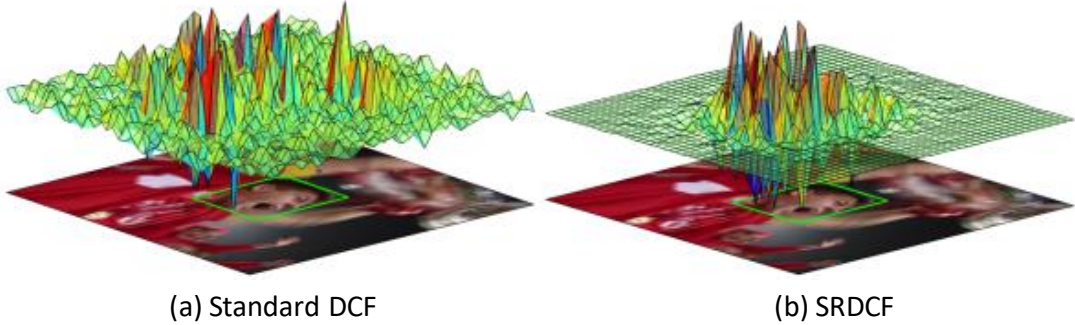


Fig. 4. Difference between standard DCF and SRDCF [27].

target appearances. Whenever a new appearance is found during tracking, a new GMM component is initialized. If the maximum limit of components is achieved, then a GMM component with minimum weight is discarded if its weight is less than a threshold value. Otherwise, the two closest components are merged into one component.

The Channel Spatial Reliability for DCF (CSRDCF) [28] tracking algorithm integrates channel and spatial reliability with DCF. Training patches also contain non-required background information in addition to the required target information. Therefore, DCFs may also learn background information, which may lead to the drift problem. In CSRDCF, spatial reliability is ensured by estimating a spatial binary map at current target position to learn only target information. Foreground and background models retained as colour histogram are used to compute appearance likelihood using Bayes' rule. A constrained CF is obtained by convolving the CF with spatial reliability map that indicates which pixels should be ignored. Channel reliability is measured as a product of channel reliability measure and detection reliability measures. The channel reliability measure is the maximum response of channel filter. Channel detection reliability in response map is computed from the ratio between the second and first major modes, clamped at 0.5. Target position is estimated at maximum response of search patch features and the constrained CF, and is weighted by channel reliability.

Mueller et al. [87] proposed Context Aware Correlation Filter tracking (CACF) framework where global context information is integrated within Scale Adaptive Multiple Feature (SAMF) [94] as baseline tracker. The model is improved to compute high responses for targets, while close to zero responses for context information. The SAMF uses KCF as baseline and solves the scaling issue by constructing a pool containing the target at different scales. Bilinear interpolation is employed to resize the samples in the pool to a fixed size template. Kiani et al. [88] exploited the background patches and proposed Background Aware Correlation Filter (BACF) tracker.

The Structuralist Cognitive model for Tacking (SCT) [89] divides the target into several cognitive units. During tracking, the search region is decomposed into fixed-size grid map, and an individual Attentional Weight Map (AWM) is computed for each grid cell. The AWM is computed from the weighted

sum of Attentional Weight Estimators (AWE). The AWE assigns more weights to target grid which less weights are given to background grid using a Partially Growing Decision Tree (PGDT) [95]. Each unit works as individual KCF with Attentional CF (AtCF), having different kernel types with distinct features and corresponding AWM. The priority and reliability of each unit are computed based on relative performance among AtCFs and its own performance, respectively. Integration of response maps of individual units gives target position.

Choi et al. proposed a Attentional CF Network (ACFN) [90] exploits target dynamic based on an attentional mechanism. An ACFN is composed of a CF Network (CFN) and Attentional Network (AN). The CFN has several tracking modules that compute tracking validation scores as precision. The KCF is used for each tracking module with AtCF and AWM. The AN selects tracking modules to learn target dynamics and properties. The AN is composed of 2 Sub Networks (SN) such as Prediction SN (PSN) and Selection SN (SSN). Validation scores for all modules are predicted in PSN. The SSN chooses active tracking modules based on current estimated scores. Target is estimated as that having the best response among the selected subset of tracking modules.

3) Siamese-Based Correlation Filter Trackers

A Siamese network joins two inputs and produces a single output. The objective is to determine whether identical objects exist, or not, in the two image patches that are input to the network. The network measures similarity between the two inputs, and has the capability to learn similarity and features jointly. The concept of Siamese network was intially used for signature verification and fingerprint recognition. Later, Siamese networks were used in various applications, including face recognition and verification [97], stereo matching [98], optical flow [99], large scale video classification [100] and patch matching [101]. We observe that Siamese architecture using CNN find similarity between two images using shared (convolutional and/or fully connected) layers. Siamese CNN can be categorized into three main groups based on late merge, intermediate merge, and early merge [96] (Fig. 5).

- Late merge: Two image patches are evaluated separately in parallel using the same network and combined at the final layer [102].
- Intermediate merge: The network processes input images

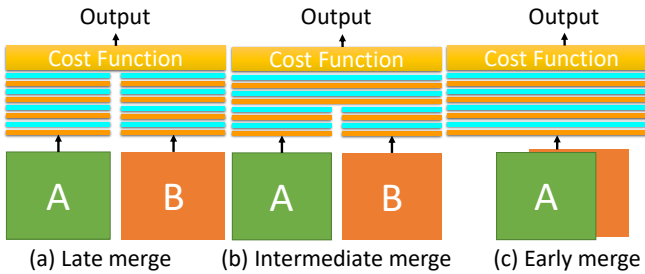


Fig. 5. Siamese CNN typologies [96].

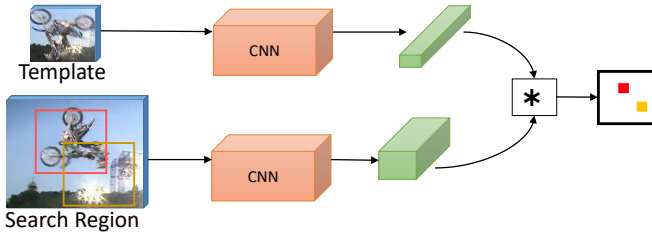


Fig. 6. The framework of SiameseFC [26].

separately and then merges into a single stream well before the final layer [99].

- Early merge: Two image are stacked and a unified input is fed to single CNN.

Integration of CFTs with Siamese network for visual tracking are classified as **Siamese-Based CFTs** and has been used to handle tracking challenges [103], [26], [104], [105], [106].

Siamese Fully Convolutional networks (SiameseFC) [26] shown in fig. 6 solves the tracking problem using similarity learning that compares exemplar (target) image with a same-size candidate image, and yields high scores if the two images are the same. The SiameseFC algorithm is fully convolutional, and its ouptut is a scalar-valued score map that takes as input an example target and search patch larger than target predicted in the previous frame. The SiameseFC network utilizes a convolutional embedding function and a correlation layer to integrate the deep feature maps of the target and search patch. Target position is estimated at maximum value in response map. This gives frame to frame target displacement. Valmadre et al. [104] introduced Correlation Filter Network (CFNet) for end-to-end learning of underlying feature representations through gradient back propagation. SiameseFC is used as base tracker, and CFNet is employed in forward mode for online tracking. During the online tracking of CFNet, target features are compared with the larger search area on new frame based on previously estimated target location. A similarity map between the target template and the search patch is produced by calculating the cross-correlation.

The Discriminative Correlation Filters Network (DCFNet) [105] utilizes lightweight CNN network with correlation filters to perform tracking using offline training. The DCFNet performs back propagation to adapt the CF layer utilizing a probability heat-map of target position.

Recently, Guo et al. [103] presented DSaim that has the potential to reliably learn online temporal appearance variations. The DSaim exploits CNN features for target appearance

and search patch. Contrary to the SiameseFC, the DSaim learns target appearance and background suppression from previous frame by introducing regularized linear regression. Target appearance variations are learned from first frame to current frame, while background suppression is performed by multiplying the search patch with the learned Gaussian weight map. The DSaim performs element-wise deep feature fusion through circular convolution layers to multiply inputs with weight map. Huang presented EArlly Stopping Tracker (EAST) [106] to learn polices using deep Reinforcement Learning (RL) and improving speedup while maintaining accuracy. The tracking problem is solved using Markov decision process. A RL agent makes decision based on multiple scales with an early stopping criterion.

4) Part-Based Correlation Filter Trackers

These kind of trackers learn target appearance in parts, while in other CFTs target template is learned as a whole. Variations may appear in a sequence, not just because of illumination and viewpoint, but also due to intra-class variability, background clutter, occlusion, and deformation. For example, an object may appear in front of the object being tracked, or a target may undergo non-rigid appearance variations. Part-based strategies are widely utilized in several applications, including object detection [107], pedestrian detection [108] and face recognition [109]. Several part-based trackers [110], [111], [112], [46], [113], [114], [115] have been developed to solve the challenges where targets are occluded or deformed in the sequences.

Real time Part based tracking with Adaptive CFs (RPAC) [110] adds a spatial constraint to each part of object as shown in Fig. 7. In RPAC, KCF tracker is employed to track individually five parts of a target. Confidence score map for each part is computed by assigning adaptive weights during tracking for every new input frame. A joint map is constructed by assigning adaptive weights to each five confidence score maps and a new target position is estimated using particle filter method. During tracking, adaptive weights or confidence scores for each part are calculated by computing sharpness of response map and Smooth Constraint of Confidence Map (SCCM). Response sharpness is calculated using Peak-to-Side-lobe Ratio (PSR), while SCCM is defined by the spatial shift of a part between two consecutive frames. Adaptive part trackers are updated for parts with weights higher then a threshold value. A Bayesian inference theorem is employed to compute the target position by calculating the Maximum A Posteriori (MAP) for all parts.

The Reliable Patch Tracker (RPT) [111] is based on particle filter framework which apply KCF as base tracker for each particle, and exploits local context by tracking the target with reliable patches. During tracking, the weight for each reliable patch is calculated based on whether it is a trackable patch, and whether it is a patch with target properties. The PSR score is used to identify patches, while motion information is exploited for probability that a patch is on target. Foreground and background particles are tracked along with relative trajectories of particles. A patch is discarded if it is no longer reliable, and re-sampled to estimate a new reliable patch. A new target position is estimated by Hough Voting-like strategy by obtaining all the weighted, trackable, and reliable

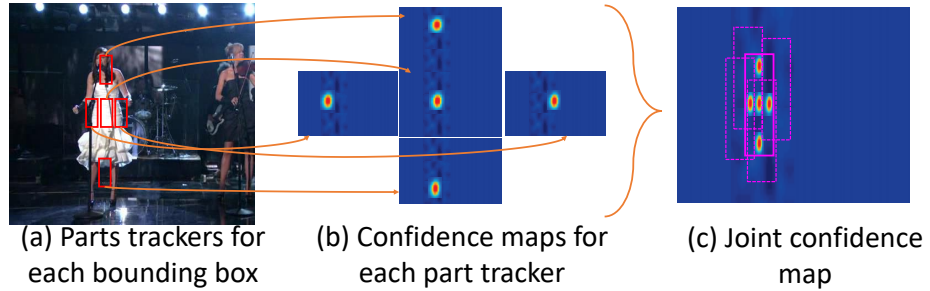


Fig. 7. Each part tracker computes response map independently. Response maps are combined to get a joint confidence map as weighted sum of individual maps in the Bayesian framework. Purple rectangles represent the sample candidates while solid purple denote the maximum likelihood on the confidence map [110].

positive patches. Recurrently Target attending Tracking (RTT) [112] learns the model by discovering and exploiting the reliable spatial-temporal parts using DCF. Quard-directional RNNs are employed to identify reliable parts from different angles as long-range contextual cues. Confidence maps from RNNs are used to weight adaptive CFs during tracking to suppress the negative effects of background clutter. Patch based KCF (PKCF) [114] is a particle filter framework to train target patches using KCF as base tracker. Adaptive weights as confidence measure for all parts based on the PSR score are computed. For every incoming frame, responses for each template patch are computed. The PSR for each patch is computed, and maximum weighted particles are selected.

The Enhanced Structural Correlation (ESC) tracker [46] exploits holistic and object parts information. The target is estimated based on weighted responses from non-occluded parts. Colour histogram model, based on Bayes' classifier is used to suppress background by giving higher probability to objects. The background context is enhanced from four different directions, and is considered for the histogram model of the object's surroundings. The enhanced image is broke down into patches (one holistic and four local) and CF is employed to all patches. The CF is employed to all image patches and final responses are obtained from the weighted response of the filters. Weight as a confidence score for each part is measured from the object likelihood map and the maximum responses of the patch. Adaptive CFs are updated for those patches whose confidence score exceeds a threshold value. Histogram model for object are updated if the confidence score of object is greater then a threshold value, while background histogram model is updated on each frame. Zuo et al.[113] proposed Structural CF (SCF) to exploit the spatial structure among the parts of an object in its dual form. The position for each part is estimated at the maximum response from the filter response map. Finally, the target is estimated based on the weighted average of translations for all parts.

5) Fusion-based Correlation Filter Trackers

In image fusion, complementary information is fused to improve performance in numerous applications including medical imaging [116], face recognition [117], image segmentation [118], and image enhancement [119]. Image fusion may be performed as Pixel-Level Fusion (PLF), Feature-Level Fusion (FLF), and Decision-Level Fusion (DLF) as shown in Fig. 8.

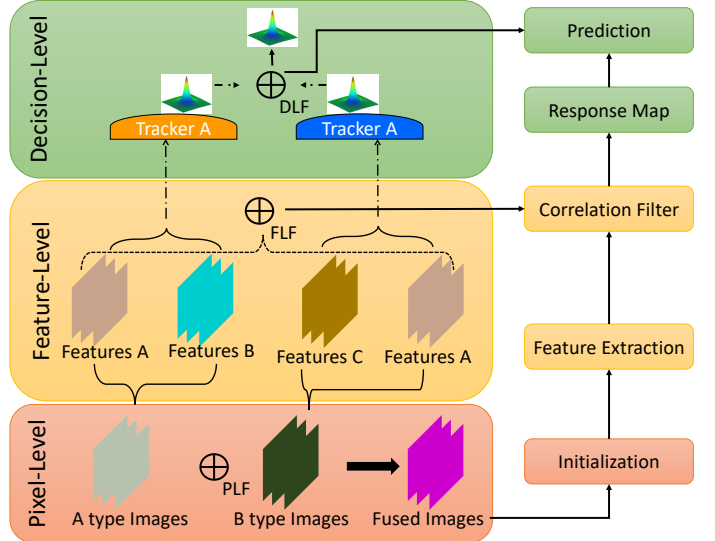


Fig. 8. Pixel-level, feature-level and decision level fusion-based tracking framework [120].

Numerous trackers using different types of fusion have been developed including [120], [121], [122], [123], [124].

Luo et al. [120] used SAMF as a baseline tracker and performed those fusions. Authors used visual and infrared images for PLF, HOG, grey while colorname features are used for FLF. Ma et al. [123] proposed FLF tracker where raw pixels, color histogram and Haar features were employed. Authors divided the region of interest into sub-parts and evaluated the features individually, which are fused using weighted entropy to exploit the complementary information. Target appearances are updated via subspace for each kind of feature with new object samples. Wang et al. [121] introduced deep feature fusion technique using two networks, Local Detection Network (LDN) and Global Network Detection (GDN). LDN employs VGG-16 and fuses the deep features extracted from conv4-3 and conv5-3 layers to generate response map. Feature map from conv5-3 is upsampled using a deconvolution layer and added to conv4-3 features. If confidence score is less then a threshold then target is considered to be lost. GDN detects the target if LDN fails to track. It employs Region Proposal Network (RPN) after conv4-3. LDN is updated to integrate

target variations while GDN parameters are fixed.

Rapuru et al. [122] proposed Correlation based Tracker level Fusion (CTF) by integrating two complementary trackers, Tracking-Learning-Detection (TLD) [125] and KCF. TLD tracker has resumption ability and is composed of three basic units, tracking to predict the new target position; target localization in current frame; rectifying the detector error by learning different target variations. KCF tracker performs tracking by detection and uses non-linear regression kernels. KCF exploits the training and testing data in circulant structure that results in low computational cost. During tracking, if the output of TLD tracker is valid then output for KCF tracker is computed. Conservative correspondence C^c for both trackers is calculated as confidence score such that the first 50% of positive patches has resemblance with the sample patches. Current bounding box (cbb) is the output of that tracker which has maximum C^c score. TLD calculates clusters of positive patches as TLD detector response (dbb). Final bounding box (fbb) is calculated as: if overlap score between cbb and dbb is greater than a threshold, and relative similarity is also greater than a threshold, otherwise the target is considered lost. Relative similarity depicts the target confidence. The fbb is computed as weighted mean of dbb and cbb .

B. Non-Correlation Filter Trackers (NCFT)

We categorize all trackers which do not employ correlation filters as **Non-Correlation Filter based Trackers** (NCFTs). We categorize NCFTs into multiple categories including patch learning, sparsity, superpixel, graph, multiple-instance-learning, part-based, and Siamese-based trackers. These trackers are discriminative except sparsity-based trackers which are generative trackers.

1) Patch Learning Trackers

Patch learning trackers exploit both target and background patches. A tracker is trained on positive and negative samples. The trained tracker is tested on number of samples, and the maximum response gives the target position. Several trackers have been proposed including [126], [127], [128], [129], [130], [131], [132], [133], [134], [135], [136], [137], [138], [139].

A Multi-Domain Network (MDNet) [126] consists of shared layers (three convolutional and two Fully-Connected (FC) layers) and one domain-specific FC layer as shown in Fig. 9. Shared layers exploit generic target representation from all the sequences, while domain specific layer is responsible for identification of target using binary classification for a specific sequence. During online tracking, the domain specific layer is independently learned at the first frame. Samples are generated based on previous target location, and a maximum positive score yields the new target position. Weights of the three convolutional layers are fixed while weights of three fully connected layers are updated for short- and long-term updates. Long-term update is performed after a fixed interval from positive samples. The short-term update is employed whenever tracking fails and the weight adaption for FC layers is performed using positive and negative samples from the current short term interval. Target position is adjusted by employing a bounding box regression model [140] in the subsequent frames.

A Structure Aware Network (SANet) [127] exploits the target's structural information based on particle filter framework. CNN and RNN deep features are computed for particles. RNN encodes the structural information of the target using directed acyclic graphs. SANet is a modified version of MDNet, with the addition of RNN layers to amplify the rich object representation. Convolutional and recurrent features are fused using a skip concatenation strategy to encode the rich information. Han et al. [128] presented Branch-Out algorithm, which uses MDNet as a base tracker. The Branch-Out architecture comprises of three CNN and multiple FC layers as branches. Some branches consists of one fully-connected layer, while others have two fully-connected layers. During tracking, a random subset of branches is selected by Bernoulli distribution to learn target appearance.

Zhang et al. [129] proposed Convolutional Networks without Training (CNT) tracker employ particle filter framework that exploits the inner geometry and local structural information of the target. The CNT algorithm is an adaptive algorithm in which appearance variation of target is adapted during the tracking. CNT employs a hierarchical architecture with two feed forward layers of convolutional network to generate an effective target representation. In the CNT, pre-processing is performed on each input image where image is warped and normalized. The normalized image is then densely sampled as overlapping local image patches of fixed size, also known as filters, in the first frame. After pre-processing, a feature map is generated from a bank of filters selected with k-mean algorithm. Each filter is convolved with normalized image patch, which is known as simple cell feature map. In second layer, called complex cell feature map, a global representation of target is formed by stacking simple cell feature map which encodes local as well as geometric layout information.

Exemplar based Linear Discriminant Analysis (ELDA) [130] employs LDA to discriminate target and background. ELDA takes several negative samples from the background and single positive sample at current target position. ELDA has object and background component models. The object model consists of long-term and short-term models. The target template at the first frame corresponds to long-term model, while short-term model corresponds to the target appearance in a short periods. The background models comprises of an online and offline background models. The online is built from negative samples around the target, while the offline background model is trained on large number of negative samples from natural images. The ELDA tracker is comprised of short and long term detectors. Target location is estimated from the sum of long-term and weighted sum of short-term detection scores. ELDA has been enhanced by integration with CNN, and named as Enhanced CNN Tracker (ECT) [131].

The Biologically Inspired Tracker (BIT) [132] performs tracking like ventral stream processing. The BIT tracking framework consists of an appearance and tracking model. The appearance model has two units, classical simple cells (S1) and cortical complex cells (C1). A S1 is responsible to exploiting colour and texture information, while a C1 performs pooling and combining of color and texture features to form complex cell. A two-layer tracking model is composed of generative

and discriminative models: a view-tuned learning (S2) unit and a task dependent learning (C2) unit. Generative S2 unit computes response map by performing convolution between the input features, and the target and response maps are fused via average pooling. The discriminative C2 unit then computes new target position by applying CNN classifier. An Action-Decision Network (ADNet) [133] controls sequential actions (translation, scale changes, and stopping action) for tracking using deep RL. The ADNet is composed of three convolutional and three FC layers. An ADNet is defined as an agent with the objective to find target bounding box. The agent is pretrained to make decision about target's movement from a defined set of actions. During tracking, target is tracked based on estimated action from network at the current tracker location. Actions are repeatedly estimated by agent unless reliable target position is estimated. Under the RL, the agent gets rewarded when it succeeds in tracking the target, otherwise, it gets penalized.

The Oblique Random forest (Obli-Raf) [135] exploits geometric structure of the target. During tracking, sample patches are drawn as particles and forwarded to an oblique random forest classifier, based on estimated target position on previous frame. Obli-Raf generates the hyperplane from data particles in a semi-supervised manner to recursively cluster sample particles using proximal support vector machine. Particles are classified as target or background, based on votes at each leaf node of the tree. Particle with maximum score will be considered as newly-predicted target position. If the maximum votes limit is less than a predefined threshold, then a new particle samples set is produced from the estimated target location. If maximum limit is achieved, the model is updated otherwise the previous model is retained.

Dual Linear Structured Support Vector Machine (DLSSVM) [137] which is the motivation of Struck [141]. Usually, classifier is trained to discriminate target from background but Struck employs kernelized structured output of the SVM for adaptive tracking. DLSSVM uses dual SSVM linear kernels as discriminative classifier for explicit high dimensional features as compared to Struck. The difference between both trackers is the selection of optimization scheme to update dual coefficients. DLSSVM employs Dual Coordinate Descent (DCD) [142] optimization method to compute a closed form solution. Another difference is that in Struck, pair of dual variables are selected and optimized while DLSSVM selects only one dual variable. Scale DLSSVM (SDLSSVM) improves the tracker by incorporating multi-scale estimation.

2) Multiple-Instance-Learning Based Trackers

Multiple-Instance-Learning (MIL) was introduced by Dietterich and is widely used in many computer vision tasks where MIL is being used for example object detection [144], face detection [145] and action recognition [146]. Various researcher have employed MIL to track targets [147], [148], [149], [150], [151], [152]. In MIL based tracking, training samples are placed in bags instead of considering individual patches, and labels are given at bags level. Positive label is assigned to a bag if it has at-least one positive sample in it and on the other hand, negative bag contains all negative samples. Positive bag may contain positive and negative instances. During training in MIL, label for instances are unknown but

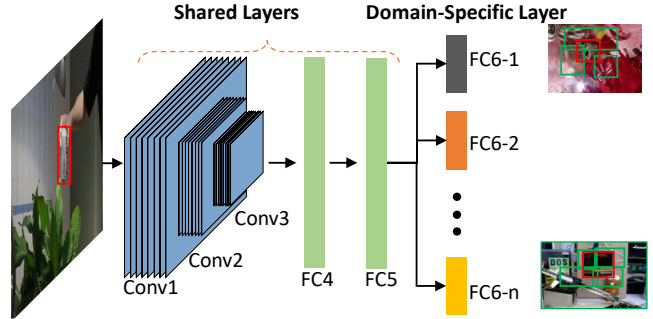


Fig. 9. MDNet architecture [126].

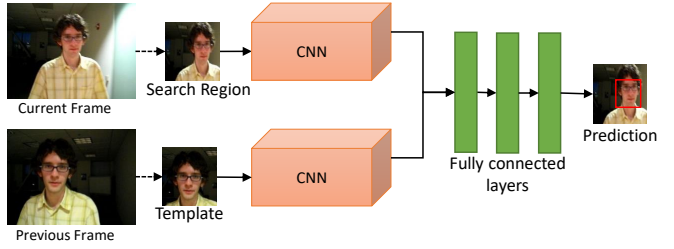


Fig. 10. GOTURN tracking framework [143].

bag labels are known. In the MIL tracking framework instances are used to construct weak classifiers and a few instances are selected and combined to form a strong classifier.

Babenko et al. [147] designed a novel MILTrack to label ambiguity of instances using Haar features. MILBoost as baseline tracker is utilized which employs the gradient boosting algorithm to maximize the log likelihood of bags. A strong classifier is trained to detect a target by choosing weak classifiers. A weak classifier is computed using log odds ratio in a Gaussian distribution. Bag probabilities are computed using a Noisy-OR model. Online boosting algorithm is employed to get new target position from weighted sum of weak classifiers.

Xu et al. [151] proposed an MIL framework that uses Fisher information using MILTrack (FMIL) to select weak classifiers. Uncertainty is measured from unlabeled samples using fisher information criterion instead of log likelihood. An online boosting method is employed for feature selection to maximize the fisher information of the bag. Abdechiri et al. [152] proposed Chaotic theory in MIL (CMIL). Chaotic representation exploits complex local and global target information. HOG and Distribution Fields (DF) features with optimal dimension are used for target representation. Chaotic approximation is employed to enhance the discriminative ability of the classifier. The significance of the instance is calculated using position distance and fractal dimensions of state space simultaneously. The appearance model known as chaotic model is learned to adapt dynamic of target through chaotic map to maximize likelihood of bags using. To encode chaotic information, state space is reconstructed by converting an image into a vector form and normalizing it with a zero mean and variance equivalent to one. Taken's embedding theory generate a multi-dimensional space map from one-dimension space.

The minimum delay in time and prediction of the embedding dimension is performed by false nearest neighbours to reduce dimensionality for state space reconstruction. Finally, GMM is imposed to model state space.

Wang et al. [148] presented Patch based MIL (P-MIL) that decomposes the target into several blocks. The MIL for each block is applied, and the P-MIL generates strong classifiers for target blocks. The average classification score, from classification scores for each block, is used to detect whole target. Sharma and Mahapatra [150] proposed a MIL tracker depends on maximizing the Classifier ScoRe (CSR) for feature selection. The tracker computes Haar-features for target with kernel trick, half target space, and scaling strategy.

Yang et al. [149] used Mahalanobis distance to compute the instance significance to bag probability in a MIL framework, and employed gradient boosting to train classifiers. Instance are computed using a coarse-to-fine search technique during tracking. The Mahalanobis distance describes the importance between instances and bags. Discriminative weak classifiers are selected based on maximum margin between negative and positive bags by exploiting average gradient and average classifier strategy.

3) Siamese Network Based NCFT Trackers

Siamese network based NCFT perform tracking based on matching mechanism. The learning process exploits the general target appearance variations. Siamese network-based trackers match target templates with candidate samples to yield the similarities between patches. Various Siamese-based CFTs have been developed including [143], [153], [154], [155], [156].

Generic Object Tracking Using Regression Network (GOTURN) proposed by Held et al. [143] exploits object appearance and motion relationships. During tracking, template and search regions are cropped at previous and current frames respectively, and those crops are padded with context information as shown in Fig. 10. Target template and search regions are fed to five individual convolutional layers. Deep features from two separate flows are fused into shared three sequential fully-connected layers. GOTURN is a feed-forward offline tracker that does not require fine-tuning, and directly regresses target location.

A Siamese INstance Search (SINT) [153] performs tracking using offline learned matching function, and finds best-matched patch between target template and candidate patches in new frames without updating matching function. The SINT architecture have two streams: a query stream and search stream. Each steam consists of five convolutional layers, three region-of-interest pooling layers, one FC layer, and a contrastive loss function layer which is responsible to discriminate target from background to fuse features. During tracking, target template as query from the initial frame is matched with candidate samples from each frame. The output bounding box is refined using four Ridge bounding box regression trained over the bounding box from the initial frame. Chen and Tao [155] proposed two flow CNN tracker called as YCNN that is learned end-to-end to calculate similarity map between the search region and the target patch using shallow and deep features. YCNN architecture has two flows: an object and

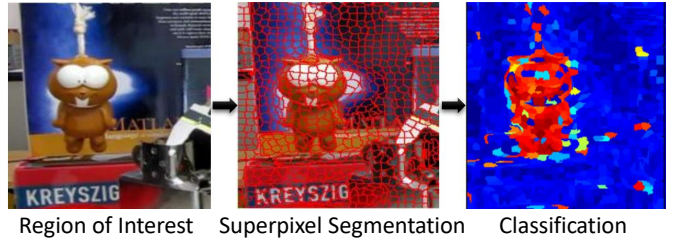


Fig. 11. Superpixel classification.

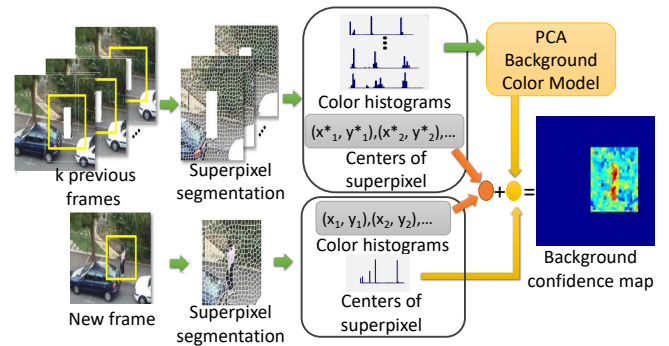


Fig. 12. BKG flowchart [157].

search flow. Deep features obtained from object and search flows having three convolutional layers are concatenated, and are forwarded to two FC layers to yield prediction map. Maximum score in the prediction map infers the new target location.

Reinforced Decision Making (RDM) [156] model is composed of a matching and a policy network. Prediction heatmaps are generated from the matching network, while the policy network is responsible for producing normalized scores from prediction heatmaps. During tracking, a cropped search patch and along with N target templates are forwarded to two separate convolutional layers and these deep features are fused using shared FC layers in matching networks to produce prediction maps. Using prediction map, policy network computes normalized scores. Prediction map gives estimated target at the maximum score. The policy network contains two convolutional and two FC layers that make decisions about a reliable state using RL.

4) Superpixel Based Trackers

Superpixels represent a group of pixels having identical pixel values [158]. Region of interest is segmented into superpixels and classification is performed over superpixels for discrimination as shown in Fig. 11. A superpixel based representation got much attention by computer vision community for object recognition [159], human detection [160], activity recognition [161], and image segmentation [158]. Numerous tracking algorithms have been developed using superpixels [162], [163], [164], [165], [157].

Li et al. [157] used BacKGround (BKG) cues in a particle framework for tracking (Fig. 12). The background is segmented excluding target area for superpixels from previous k frames. These superpixels are considered representing the background. Superpixels are also computed in the current

frame and compared with the background superpixels using Euclidean distance and color histograms. Current frame superpixels dissimilar to the background superpixels are considered as the target superpixels.

Yang et al. [165] also proposed a SuperPixel based Tracker (SPT). Mean shift clustering is performed on superpixels to model target and the background appearance. Similarity of superpixels in the current frame is computed from the target and the background models to find the target position. The Constrained Superpixel Tracking (CST) [163] algorithm employs graph labeling using superpixels as nodes and enforces spatial smoothness, temporal smoothness, and appearance fitness constraints. Spatial smoothness is enforced by exploiting the latent manifold structure using unlabeled and labeled superpixels. Optical flow is used for the temporal smoothness to impose short-term target appearance, while appearance fitness servers as long-term appearance model to enforce objectness. Wang et al. [164] presented a Bayesian tracking method at coarse-level and fine-level superpixel appearance model. The coarse-level appearance model computes few superpixels such that there is only one superpixel in the target bounding box, and a confidence measure defines whether that superpixel corresponds to background/target. The fine-level appearance model calculates more superpixels in the target region based on target location in the previous frame and Jaccard distance is used to find fine-superpixels belonging to the target in the current frame. The Structural Superpixel Descriptor (SSD) [162] exploits the structural information via superpixels and preserves the intrinsic target properties. It decomposes a target into a hierarchy of different sized superpixels and assigns greater weights to superpixels closer to the target center. A particle filter framework is used and background information is alleviated through adaptive patch weighting.

5) Graph Based Trackers

A graph has vertices (which may be pixels, superpixels or object parts) and edges (correspondence among vertices). Graphs are used to predict the labels of unlabeled vertices. Graph based algorithms have been successfully used for object detection [168], human activity recognition [169], and face recognition [170]. Generally, graph-based trackers use superpixels as nodes to represent the object appearance, while edges represent the inner geometric structure. Another strategy is to construct graphs among the parts of objects in different frames. Many trackers have been developed using graphs [171], [172], [173], [166], [174].

The Tree structure CNN (TCNN) [166] tracker employed CNN to model target appearance in tree structure. Multiple hierarchical CNN-based target appearance models are used to build a tree where vertices are CNNs and edges are relations among CNNs (Fig. 13). Each path maintains a separate history for target appearance in an interval. During tracking, candidate samples are cropped at target location estimated in the last frame. Weighted average scores computed using multiple CNNs are used to calculate objectness for each sample. Reliable patch along the CNN defines the weight of CNN in the tree structure. The maximum score from multiple CNNs is used to estimate target location. Bounding box regression methodology is also utilized to enhance the estimated target

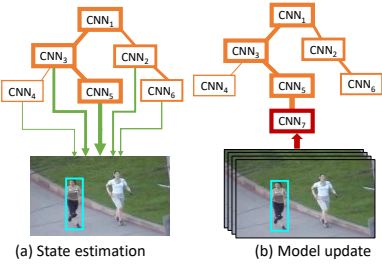


Fig. 13. Visualization of (a) target state estimation and (b) model update in Tree Structure CNN [166]. CNN weights are shown using green arrows width for state estimation. Affinity among CNNs is shown by the width of orange edge for model update while reliability of CNN is indicated by the width of CNN box.

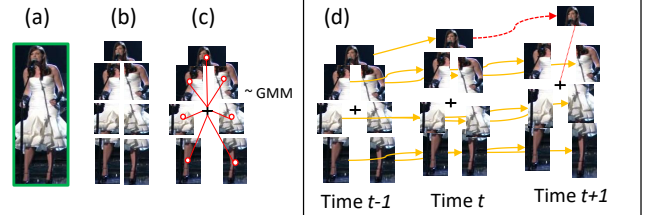


Fig. 14. ALMM tracking approach [167]. (a) Target detection. (b) Target patches extracted from input image. (c) Target patches to follow GMM based on distance of patches from center of gravity. (d) ALMM prune out patches to make robust estimation.

position in the subsequent frames.

Du et al. [172] proposed Structure Aware Tracker (SAT) that constructs hypergraphs in temporal domain to exploit higher order dependencies. SAT gathers candidate parts in frame buffer from each frame by computing superpixels. A graph cut algorithm is employed to minimize the energy to produce the candidate parts. A Structure-aware hyper graph is constructed using candidate parts as nodes, while hyper edges denote relationship among parts. Object parts across multiple frames contribute to build a subgraph by grouping superpixels considering both appearance and motion consistency. Finally, the target location and boundary is estimated by combining all the target parts using coarse-to-fine strategy. Graph tracker (Gracker) [171] uses undirected graphs to model planar objects and exploits the relationship between local parts. Search region is divided into grids, and a graph is constructed where vertices represent cells with maximum SIFT response and edges are constructed using Delaunay triangulation. During tracking, geometric graph-matching is performed to explore optimal correspondence between graph models and the candidate graph.

A Geometric hyperGraph Tracker (GGT) [173] constructs geometric hypergraphs by exploiting higher order geometric relationships among target parts. Target parts in previous frame are matched with candidate parts in new frame. The relationship between target and candidate parts is represented by correspondence hypothesis. A geometric hypergraph is constructed from the superpixels where vertices are correspondence hypothesis while edges constitute the geometric relationship within the hypothesis. Reliable parts are computed from correspondence hypotheses learned from the matched target and candidate part sets. During tracking, reliable parts are extracted with high confidence to predict target location.

An Absorbing Markov Chain Tracker (AMCT) [174] recursively propagates the predicted segmented target in subsequent frames. AMCT has two states: an absorbing and a transient state. In an AMCT, any state can be entered to absorbing state, and once entered, cannot leave, while other states are transient states. A graph is constructed between two consecutive frames based on superpixels, where vertices are background superpixels (represents absorbing states) and target superpixels (transient states). Edges weights are learned from SVM to distinguish foreground and background superpixels. Motion information is imposed by spatial proximity using inter-frame edges. The target is estimated from the superpixel components after vertices have been evaluated against the absorption time threshold.

6) Part-Based NCFT Trackers

Part-based modeling have been activity used in NCFTs to handle deformable parts. Various techniques are employed to perform object detection [175], action recognition [176], and face recognition [177] using parts. Object local parts are utilized to model a tracker [167], [178], [179], [180], [181].

Adaptive Local Movement Modeling (ALMM) [167] exploits intrinsic local movements of object parts for tracking. Image parts are estimated using a base tracker such as Struck [182], and GMM is used to prune out drifted parts. GMM is employed to model the parts movement based on displacement of centers from the global object center (Fig. 14). Each part is allocated a weight, based on motion and appearance for better estimation. The target position is estimated from a strong tracker by combining all parts trackers in a boosting framework.

Yao et al. [178] proposed a Part based Tracker (PT) where object is decomposed into parts and each part is assigned an adaptive weight. A structural spatial constraint is applied to each part using minimum spanning tree where vertices represents parts and edges define consistent connections. A weight is assigned to each edge corresponding to Euclidean distance between two parts. Online structured learning using SVM is performed to distinguish target and its parts from background. During tracking, the maximum classification scores of target and parts estimates the new target position.

Li et al. [180] used local covariance descriptors as target appearance and exploited the relationship among parts. The target is divided into non overlapping parts. A pyramid is constructed having multiple local covariance descriptors are fused using max pooling depicting target appearance. Parts are modeled using star graph and central part of target representing central node. During tracking, target parts are selected from candidate part pools and template parts by solving linear programming problem. Target is estimated from selected parts using weighted voting mechanism based on relationship between centre part and surrounding parts. Part-based Multi-Graph Ranking Tracker (PMGRT) [179] constructs graphs to rank target parts. During tracking, target is divided into parts and different features are extracted for each target part. Multiple graphs are constructed based on both target parts and feature types, where one graphs is from one feature type. An affinity weight matrix is formed where rows represents graphs for different features and columns denotes the graphs of

various parts. Augmented Lagrangian formulation is optimized to select parts associated with high confidence.

7) Sparsity Based Trackers

All algorithms studied so far are discriminative tracking methods. On the other hand, Generative methods learn target representation and search target in each frame with minimal reconstruction error [37]. Sparse representation is a good example for generative models. Sparse representations are widely in computer vision, signal processing, and image processing communities for numerous applications such as face recognition [183], object detection [184], and image classification [185]. The objective is to discover an optimal representation of the target which is sufficiently sparse and minimizes the reconstruction error. Mostly sparse coding is performed by first learning a dictionary. Assume $\mathbf{X} = [x_1, \dots, x_N] \in \mathcal{R}^{m \times n}$ represents gray scale images $x_i \in \mathcal{R}^m$. A dictionary $\mathbf{D} = [d_1, \dots, d_k] \in \mathcal{R}^{m \times k}$ is learned on \mathbf{X} such that each image in \mathbf{X} can be sparsely represented by a linear combination of items in \mathbf{D} : $x_i = \mathbf{D}\alpha_i$, where $\alpha_i = [\alpha_1, \dots, \alpha_k] \in \mathcal{R}^k$ denotes the spares coefficients. When $k > r$, where r is the rank of \mathbf{X} , then dictionary \mathbf{D} is overcomplete. For a known \mathbf{D} , a constrained minimization using ℓ_1 -norm is often applied to find α for sufficiently sparse solution:

$$\alpha_i^* \equiv \arg \min_{\alpha_i} \frac{1}{2} \|x_i - \mathbf{D}\alpha_i\|_2^2 + \lambda \|\alpha_i\|_1, \quad (3)$$

where λ gives relative weights to the sparsity and reconstruction error. Dictionary \mathbf{D} is learned in such a way that all images in \mathbf{X} can be sparsely represented with a small error. Dictionary \mathbf{D} is learned to solve following optimization problem:

$$\{\alpha^*, \mathbf{D}^*\} \equiv \underset{\mathbf{D}, \alpha}{\text{minimize}} \sum_{i=1}^N \|\mathbf{X} - \mathbf{D}\alpha\|_2^2 + \lambda \|\alpha\|_1, \quad (4)$$

There are two alternative phases for dictionary learning. \mathbf{D} is assumed to be fixed and the coefficients α are calculated in the initial phase. While in the second phase, dictionary \mathbf{D} is updated while α is assumed to be fixed. In visual object tracking, the objective of dictionary learning is to perform discrimination between target and background patches by sparsely encoding target and background coefficients. Various sparsity based trackers have been proposed including [186], [187], [188], [189], [190], [191].

Structural sparse tracking (SST) [186] is based on particle filter framework which exploits intrinsic relationship of local target patches and global target to jointly learn sparse representation. Fig. 15 presents different types of sparse representations of target. Fig 15 (a) shows global sparse representation which exploits holistic representation of the target and is optimized using ℓ_1 minimization [192]. Local sparse representation models present the target patches sparsely in local patch dictionary as shown in Fig. 15 (b) [193]. The joint sparse representation exploits the intrinsic correspondence among particles to jointly learn the dictionaryay [194] (Fig. 15 (c)). Joint sparsity enforces particles to be jointly sparse and share the same dictionary template. SST exploits all the three sparse representations in a unified form as shown in Fig. 15 (d). SST estimates target from target dictionary templates and corresponding patches having maximum similarity score from all the particles by preserving the spatial layout structure. The

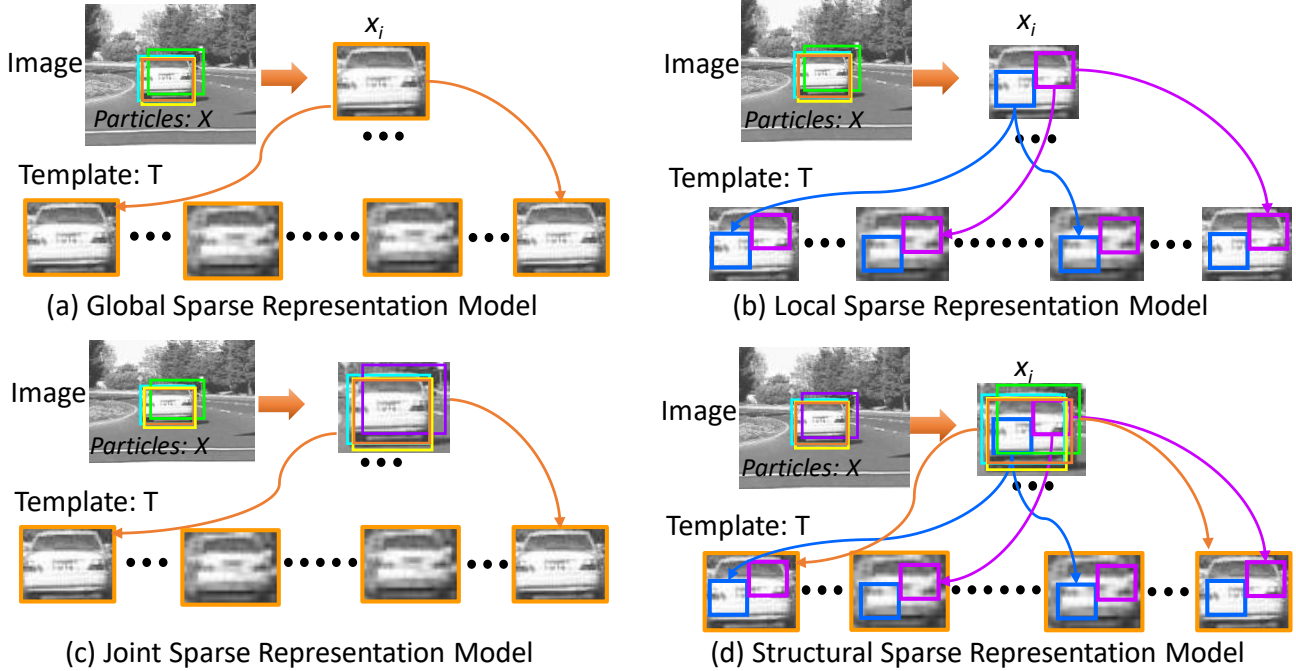


Fig. 15. (a) global sparse representation [192], (b) local sparse representation model [193], (c) joint sparse representation model [194] and (d) structural sparse representation model [186].

model is constructed on a number of particles representing target, and each target representation is decomposed into patches, and dictionary is learned. The patch coefficient is learned such that it minimizes the patch reconstruction error. SST considers the same local patches from all the particles are similar. But this is not the case for tracking because usually outliers exist. Another problem in SST is that some local patches can select different target templates due to noise or occlusion. Zhang et al. [187] improved SST and proposed Robust Structural Sparse Tracking (RSST) to exploit the shared correspondence by the local patches and also modeled the outliers because of noise and occlusion.

Context aware Exclusive Sparse Tracker (CEST) [190] exploits context information utilizing particle filter framework. The CEST performs linear combination of dictionary elements to represent particles. Dictionary is modeled as groups containing target, occlusion and noise, and context templates. In particle framework, new target is estimated as best particle from target template dictionary. Guo et al. [188] computed weight maps to represent target and background structure. A reliable structural constraint is imposed using the weight maps by penalizing the occluded target pixels. Using a Bayesian filtering framework, target is estimated using maximum likelihood from the estimated object state for all the particles. Yi et al. [189] proposed Hierarchical Sparse Tracker (HST) to integrate the discriminative and generative models. The proposed appearance model is comprised of Local Histogram Model (LHM), Sparsity based Discriminant Model (SDM), and Weighted Align Pooling (WAP). LHM encodes the spatial information among target parts while the WAP assigns weights to local patches based on similarities between target

and candidates. The target template sparse representation is computed in SDM. Finally, candidate with the maximum score from LHM, WAP, and SDM determines the new target position.

In this section we have studied CFTs and NCFTs and elaborated different tracking frameworks and classified trackers into different subcategories. We summarized the characteristics of important well-cited trackers from each subcategory in Table I.

IV. EXPERIMENTS AND ANALYSIS

We have performed exhaustive experiments on three publicly available visual object tracking benchmarks including OTB2013 [7], OTB2015 [8], and TC-128 [195]. We also evaluated these trackers on our newly introduced benchmark **Object Tracking and Temple Color** (OTTC) as explained in Section IV-A. First, we give brief introduction of selected benchmarks, evaluation protocols and selected trackers for comparison. Then, we report a detailed analysis of experimental study performed over selected benchmarks and provide our insights and findings. A project page containing more experimental details and results will soon be made publicly available .

A. Benchmarks

OTB2013 [7] contains 50 sequences which are divided into 11 different challenges including Motion Blur (MB), Occlusion (Occ), Deformation (DEF), In-Plane Rotation (IPR), Fast Motion (FM), Low Resolution (LR), Scale Variation (SV), Background Clutter (BC), Out-of-View (OV), Illumination Variation (IV), and Out-of-Plane Rotation (OPR). **OTB2015** [8] is an improved version of OTB2013 consisting of 100

TABLE I
CFTs AND NCFTs, AND THEIR CHARACTERISTICS.

Category	Subcategory	Tracker	Features	Baseline tracker	Scale estimation	Offline training	Online learning	FPS	Benchmarks	Publication	year
CFTs	Basic	KCF	HOG, Raw pixels	No	No	Yes	172	OTB2013		TPAMI	2015
		CF2	None	KCF	No	No	Yes	10.4	OTB2013, OTB2015	ICCV	2015
		HDT	CNN	KCF	No	No	Yes	10	OTB2013, OTB2015	CVPR	2016
		LCT	HOG	KCF	Yes	No	Yes	27.4	OTB2013	CVPR	2015
		fDST	HOG	DCF	Yes	No	Yes	54.3	OTB2013, VOT2014	TPAMI	2015
	R-CFTs	Staple	HOG, Color Histogram	KCF	Yes	No	Yes	80	OTB2013, VOT14, VOT2015	CVPR	2016
		SRDCF	HOG, CN		No	No	Yes	5	OTB-2013, OTB-2015, ALOV++ and VOT2014	ICCV	2015
		CCOT	CNN	CCOT	Yes	No	Yes	0.3	OTB2015, Temple-Color, VOT2015	ECCV	2016
		ECO	CNN, HOG, CN	CCOT	Yes	No	Yes	8	OTB2015, UAV123, OTB2015, TempleColor	CVPR	2017
		CSRDCF	HOG, Colornames, color histogram	SAMF	Yes	No	Yes	13	OTB2015, VOT2015, VOT2016	CVPR	2017
Part-based	Siamese-based	CACF	HOG	KCF	Yes	No	Yes	13	OTB2013, OTB2015	CVPR	2017
		SCT	HOG, RGB, colornames	KCF	No	No	Yes	40	OTB2013	CVPR	2016
		SiameseFC	CNN	SiameseFC	Yes	Yes	No	58	OTB2013, VOT2014, VOT2015, VOT2016	ECCV	2016
		CFNet	CNN	SiameseFC	Yes	Yes	Yes	43	OTB2013, OTB2015, VOT2014, VOT2016, TempleColor	CVPR	2017
		Daum	CNN	SiameseFC	Yes	Yes	Yes	45	OTB2013, OTB2015	ICCV	2017
	EAST	HOG, raw pixels, CNN			Yes	Yes	Yes	23	OTB2013, OTB2013, VOT2014, VOT2015	CVPR	2017
		RPCF	HOG	KCF	Yes	No	Yes	30	selected Sequences	CVPR	2015
		RPT	HOG	KCF	No	No	Yes	4	OTB2013 and 10 selected sequences	CVPR	2015
		RTT	HOG, RNN	KCF	Yes	Yes	Yes	3.5	OTB2013	CVPR	2016
		PKCF	HOG, CN	KCF	Yes	No	Yes	0.5	OTB2013	Neurocomputing	2016
Non-CFTs	Fusion-based	Ma's	pixels, color histogram, Haar features		Yes	No	Yes	0.4		ICCV	2015
		Wang's	CNN		Yes	Yes	Yes	13	Selected sequences	ICASSP	2017
		CFP	Haar, binary features	KCF, TLD	Yes	Yes	Yes	25	AUC(300+), OTB2013, VOT2015	TIP	2017
		MDNet	CNN	MDNet	Yes	Yes	Yes	1	OTB2013, OTB2015, VOT2014	CVPR	2016
		SANET	CNN, RNN		Yes	Yes	Yes	1	OTB2015, TempleColor, VOT2015	CVPR	2017
	Patch learning	CNT	raw pixels		No	No	Yes	1.5	OTB2013	TIP	2016
		ADNet	CNN		Yes	Yes	Yes	3	OTB2013, OTB2015, VOT2013, VOT2014, VOT2015, ALOV300++	CVPR	2017
		DRL	CNN, RNN		Yes	No	Yes	45	OTB2013, OTB2015	arXiv	2017
		Obli-Raf	CNN, HOG		Yes	No	Yes	2	OTB2013, OTB2015	CVPR	2017
		SDLSVM	LRT (low Rank Transform)	Struck	Yes	No	Yes	5.4	OTB2013, OTB2015	CVPR	2016
Non-CFTs	MIL	DeepTrack	CNN		Yes	Yes	Yes	2.5	OTB2013, OTB2013	TIP	2016
		MILTrack	Haar	MILBoost	Yes	No	Yes	25	Selected Sequences	TPAMI	2011
		FMIL	Haar	MILBoost	Yes	No	Yes	50	12 Selected Sequences	Pattern Recognition	2015
		CMI	HOG, Distribution Field		No	No	Yes	22	20 Selected Sequences	Neurocomputing	2017
		SST	gray scale	SST	Yes	No	Yes	0.45	20 Selected Sequences	CVPR	2015
	Sparsity-based	gray scale	HOG and CNN	SST	Yes	No	Yes	1.8	OTB2013, OTB2013, OTB2013, OTB2015 and VOT2014	TPAMI	2018
		GRST	gray scale, HOG and CNN	SST	Yes	No	Yes	4.77	15 Selected Sequences	T-CYBERNETICS	2016
		Siamese-based	GOTURN	CNN	Yes	Yes	No	100	VOT2014	ECCV	2016
		SINT	CNN		Yes	Yes	No	OTB2013	CVPR	2016	
		VCNN	CNN		Yes	Yes	No	45	OTB2015, VOT2014	T-CVST	2017
Non-CFTs	Superpixel	BKG	HSI color histogram		Yes	No	Yes	0.77	12 Selected sequences	T-CVST	2014
		SPT	HSI color histogram		Yes	No	Yes	5	12 Selected sequences	TIP	2014
		GRST	CNN		Yes	No	Yes	1.5	OTB2013, OTB2015, VOT2015	arXiv	2016
		Graph	SAT		Yes	No	Yes	0.5	Defom-SOT	TIP	2016
		Part-based	ALMM	Haar, Raw pixels, Histogram features	Stuck	No	No	Yes	40	OTB2013, 57 Selected Sequences	T-CVST
	Part-based	PT	Haar Features		No	No	Yes	2.5	13 Selected Sequences	TPAMI	2017

TABLE II
DETAILS OF DIFFERENT BENCHMARKS.

Benchmarks	OTB2013	OTB2015	TC-128	OTTC	VOT2017
Sequences	50	100	128	186	60
Min frames	71	71	71	71	41
Max frames	3872	3872	3872	3872	1500
Total frames	29491	59040	55346	92023	21356

sequences and covering the same 11 challenges. **TC-128** [195] is another benchmark comprising of 128 sequences distributed over the same 11 challenges. We combined all the sequences from OTB2015 and TC-128 to form a more challenging benchmark, named as Object Tracking and Temple Color (**OTTC**). The new benchmark is a union of unique sequences from OTB2015 and TC-128 avoiding repetitions. OTTC contains 186 sequences distributed over 11 challenges. Tracking performances varies depending upon the number of sequences and the length of each sequence. Since OTB2015 and TC-128 contained 42 common sequences, a benchmark contained each sequence only once was needed to evaluate the tracking performance in a more comprehensive way. Table II shows some details of these benchmarks. We also report results over Visual Object Tracking (VOT2017) [19] benchmark which covers only five challenges including size change, occlusion, motion change, illumination change, and camera motion. Note that these challenges are more elaborately covered by OTTC benchmark, though using slightly different challenge names. Nevertheless, VOT is an important benchmark due to inclusion of very small target tracking and IR sequences.

B. Evaluation Protocols

We employed three metrics including precision, success and speed for comparison. We have evaluated the robustness of the tracking algorithms using traditional One Pass Evaluation (OPE) technique. Precision and success plots are drawn to

examine the performance of trackers. For precision, the Euclidean distance is computed between the estimated centers and ground-truth centers as: $\delta_{gp} = \sqrt{(x_g - x_p)^2 + (y_g - y_p)^2}$, where (x_g, y_g) represents ground truth center location, and (x_p, y_p) is the predicted target center position in a frame. If δ_{gp} is less than a threshold than that frame is considered as a successful. In the precision plot, the threshold δ_{gp} is fixed 20 pixels. Precision does not give a clear picture of estimated target size and shape because center position error quantifies the pixel difference. Therefore, a more robust measure known as success has often been used. For success, an Overlap Score (OS) between ground truth and the estimated bounding boxes is calculated. Let r_g be the ground-truth bounding box and r_t be the target bounding box. An overlap score is defined as: $o_s = \frac{|r_t \cap r_g|}{|r_t \cup r_g|}$, where \cap and \cup denotes the intersection and union of two regions respectively, while $|\cdot|$ represents the number of pixels. OS is used to determine whether a tracking algorithm has successfully tracked a target in the frame. Those frames having o_s scores greater than a threshold, are referred as successful frames. In the success plot, the threshold value t_0 varies between 1 and 0, hence producing varying resultant curves. OS threshold t_0 value is set at 0.5 for evaluation. We reported precision and success curves as Area under the curve (AUC). We also reported the speed of the trackers in Frames Per Second (FPS). FPS is the average speed of the trackers over all the sequences in a benchmark.

C. Tracking Algorithms

We have selected 24 trackers proposed over the last 4 years having error-free easily executable codes (table III). Selected trackers include CSRDCF [28], STRCF [84], deep-SDRDCF [24], CF2 [66], DCFNet [105], BACF [88], ECO [25], CCOT [86], CFNet [104], CNT [129], KCF [63], HDT [68], ECT [131], Obli-Raf [135], MCPF [71], SiameseFC

TABLE III

DETAILED INFORMATION OF SELECTED TRACKERS INCLUDING CATEGORY, FEATURES, FPS COMPUTED OVER OTTC BENCHMARK, IMPLEMENTATION DETAILS AND RESOURCE LINK. ABBREVIATIONS ARE AS FOLLOWS: BASIC (B), REGULARIZED (R), SIAMESE (S), PART BASED (PB), PATCH LEARNING (PL), INTENSITY ADJUSTED HISTOGRAM (IAH), PIXEL INTENSITY HISTOGRAM (PIH), COLOR NAMES (CN), COLOR HISTOGRAM (CH), MATLAB (M), AND MATCONVNET (M) [196].

Trackers	Category	Feature	FPS	Implementation	GPU	Resource Link
CSRDCF	R-CFT	HOG, CN, Gray	8.17	M	No	https://github.com/alanlukezic/csr-dcf
ECO	R-CFT	CNN, HOG, CN	6.72	M+m	Yes	https://github.com/martin-danelljan/ECO
CCOT	R-CFT	CNN	0.41	M+m	Yes	https://github.com/martin-danelljan/Continuous-ConvOp
STRCF	R-CFT	HOG, CN, Gray	19.03	M	No	https://github.com/lifeng9472/STRCF
MCPF	B-CFT	CNN	0.15	M+m	Yes	http://nlpr-web.ia.ac.cn/mmc/homepage/tzzhang/mcpf.html
SRDCF	R-CFT	HOG, CN	3.78	M	No	https://www.cs.tut.fi/ptv/tracker/objrec/visualtracking/regvistrack/
DCFNet	S-CFT	CNN	1.72	M+m	Yes	https://github.com/foolwood/DCFNet#dcfnet-discriminat-correlation-filters-network-for-visual-tracking
deepSRDCF	R-CFT	CNN	1.62	M+m	Yes	https://www.cvl.isy.liu.se/research/objrec/visualtracking/regvistrack/
BACF	R-CFT	HOG	18.49	M	No	http://www.hamedkiani.com/bacf.html
SRDCFdecon	R-CFT	HOG	1.48	M	No	https://www.cvl.isy.liu.se/research/objrec/visualtracking/decontrack/index.html
CF2	B-CFT	CNN	7.01	M+m	Yes	https://sites.google.com/site/jhuang0604/publications/cf2
DLSSVM	PL	IAH, RGB Image	5.92	M	No	http://www4.comp.polyu.edu.hk/~cslzhang/DLSSVM/DLSSVM.htm
HDT	B-CFT	CNN	5.68	M+m	Yes	https://sites.google.com/site/yuankiqu/hdt/
RPT	PB-CFT	HOG	6.27	M	No	https://github.com/ihpdep/rpt
ECT	PL	CNN	0.4	M+m	Yes	https://sites.google.com/site/changxingao/ecnn
ILCT	B-CFT	HOG, PIH, IAH	19.29	M	No	https://sites.google.com/site/chaoma99/cf-lstm
SiameseFC	S-CFT	CNN	24.8	M+m	Yes	http://www.robots.ox.ac.uk/~luca/siamese-fc.html
CFNet	S-CFT	CNN	13.64	M+m	Yes	http://www.robots.ox.ac.uk/~luca/cfnet.html
STAPLE	B-CFT	HOG, CH	6.35	M	No	https://github.com/bertinetto/staple
fDSST	B-CFT	HOG	65.8	M	No	http://www.cvl.isy.liu.se/en/research/objrec/visualtracking/scalvistrack/index.html
Obliv-Raf	PL	CNN	1.73	M+m	Yes	https://sites.google.com/site/zhangueste/incremental-oblique-random-forest
KCF	B-CFT	HOG	80.85	M	No	http://www.robots.ox.ac.uk/~joao/circulant/
CNT	PL	Image Pixels	0.46	M	No	http://faculty.ucmerced.edu/mhyang/project/cnt/
BIT	PL	Gabor, CN	37.02	M	No	http://caibolun.github.io/BIT/index.html

[26], SRDCF [27], SRDCFdecon [83], STAPLE [73], fDSST [72], DLSSVM [137], ILCT [70], RPT [111], and BIT [132]. Moreover, the selected trackers are popular among the research community and are often compared on publicly available benchmarks. Most of the trackers do not require any pre-training and easy to execute without any technical difficulty. However, SiameseFC, CFNet, and DCFNet require pre-training but tested without offline training. All codes are executed by using default parameters as suggested by the original authors. We have presented both quantitative and qualitative analysis of all the compared trackers.

D. Quantitative Evaluation

1) Precision and Success

The performance of trackers is reported in terms of average precision and success (Fig. 16) on four benchmarks including OTB2013, OTB2015, TC-128 and OTTC. The performance of all the compared trackers in terms of average precision is shown in Fig. 16 (a)-(d). On OTB2013, where six trackers including CSRDCF, ECO, CCOT, STRCF, MCPF, and SRDCF obtained the average precision more than 80% while the performance of the remaining trackers degraded (Fig. 16 (a)). Similarly, over OTB2015, the same six trackers obtained a precision score of 85% or above. These 6 trackers, except MCPF, are regularized CFTs, while MCPF is a basic CFT. Four trackers including BACF, SRDCFdecon, DCFNet, deepSRDCF obtained a precision score of 80% or above whereas the remaining 14 trackers achieved less than 80% average precision. On TC-128 benchmark, majority of the trackers showed degraded performance (average precision less than 75%) while only four trackers ECO, CCOT, MCPF, and SRDCF achieved relatively better performance, {78.3%, 77.1%, 76.9%, and 75.7%} respectively (Fig. 16 (c)). The OTTC benchmark has been proved to be the most challenging benchmark, with only three trackers including ECO, CCOT,

and MCPF achieved more than 80% average precision (Fig. 16 (d)).

The success plots for four benchmarks are shown in Fig. 16 (e)-(h). Only four trackers including ECO, CSRDCF, CCOT, and STRCF obtained the average OS {63.6%, 62.6%, 61.8%, and 60.5%} on OTB2013, while the remaining 20 trackers showed a degraded average OS of less than 60.0% (Fig. 16 (e)). The best performing trackers are regularized CFTs. On OTB2015 (Fig. 16 (f)), 10 trackers attained significant improvement in terms of average OS (more than 60.0%) while the remaining trackers showed degraded performance. In contrast, none of the compared trackers achieved an average OS of more than 60.0% on TC-128 benchmark (Fig. 16 (g)). In case of OTTC benchmark, only ECO and CCOT performed better (OS 61.5% and 60.1%) while the other compared trackers achieved less than 60% OS (Fig. 16 (h)). Overall, the ECO obtained the first rank in all of the four benchmarks using both precision and success. The CNT obtained the lowest rank in both OTB2013 and OTB2015 while the SiameseFC attained the lowest rank in TC-128 and OTTC benchmarks (Figs. 16 (e)-(h)). The ECO and the CCOT showed best performance because of the contextual information preserved by using multi-resolution deep features. Most of the best performing trackers are regularized CCOTs.

We observe that a better performing tracker on one benchmark may not maintain its ranking on the other benchmarks. For example, CSRDCF and CCOT change their ranking in different benchmarks. CSRDCF performed better than CCOT on OTB2013 while CCOT performed better on the other three benchmarks (Fig. 16). The number of sequences and distribution of challenges in a benchmark may change the ranking of a tracker. As OTB2015, TC-128 and OTTC has more number of sequences therefore ranking may change significantly. Tracking performance is also affected by the number of frames in a sequence. Trackers with poor target

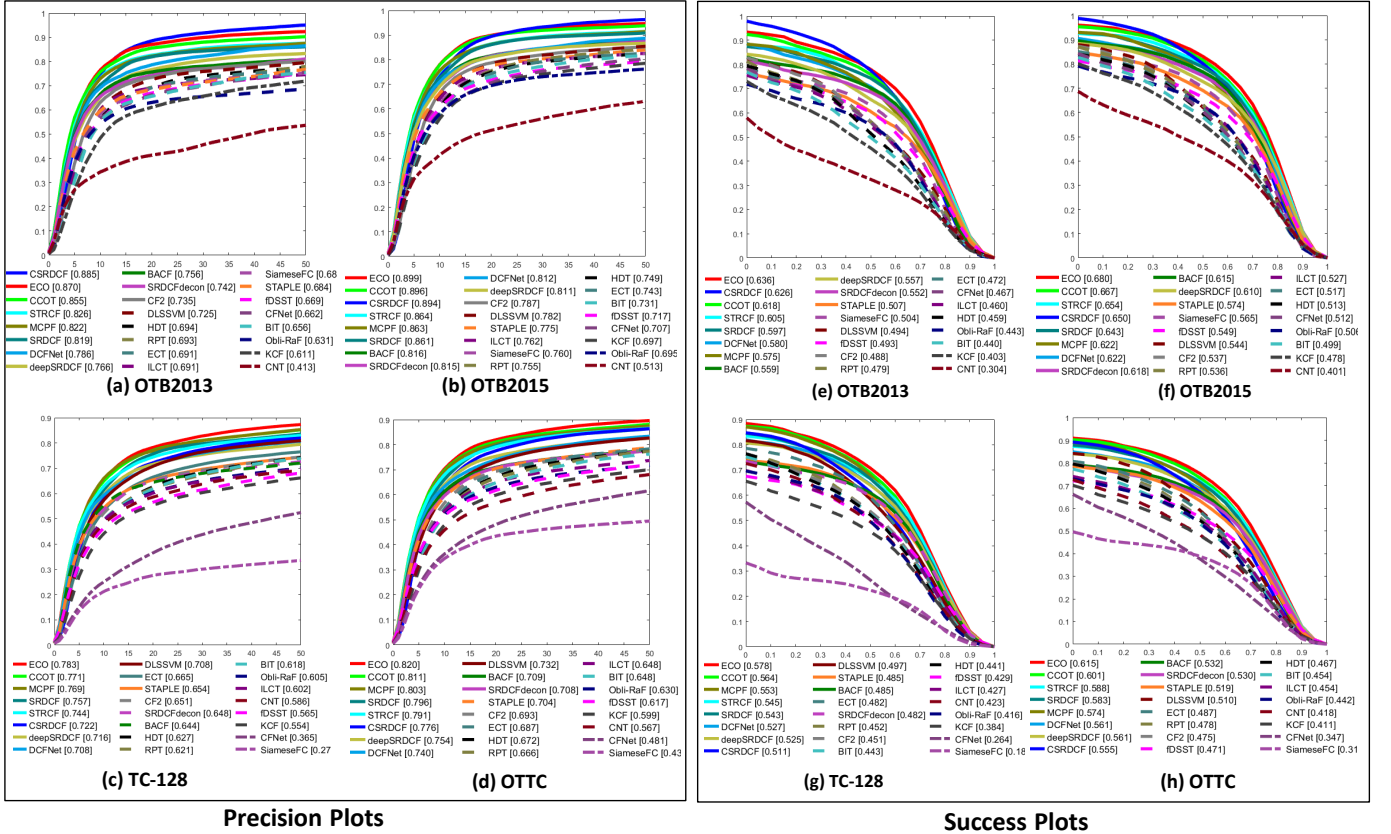


Fig. 16. Precision plots for the 24 selected trackers over (a) OTB2013, (b) OTB2015, (c) TC-128, and (d) OTTC benchmarks. Success plots over (e) OTB2013, (f) OTB2015, (g) TC-128, and (h) OTTC benchmarks are also shown.

update can only perform well over shorter sequences. If a sequence has more frames then performance on that particular sequence may degrade due to noisy update of the tracker.

2) Features based Comparison

VOT requires a rich representation of the target appearance based on different types of features. We classify the aforementioned 24 trackers into two categories. The first category comprises of those trackers which are based on HandCrafted (HC) features such as CSRDCF [28], STRCF [84], SRDCF [27], SRDCFdecon [83], BACF [88], DLSSVM [137], STAPLE [73], ILCT [70], RPT [111], BIT [132], fDSST [72], KCF [63], and CNT[129]. While the second category consists of deep feature based trackers including deepSRDCF [24], CF2[66], DCFNet [105], ECO[25], CCOT [86], CFNet [104], HDT[68], ECT [131], Obli-Raf [135], MCPF [71], and SiameseFC [26]. We used the default features setting as proposed by the original authors.

Figs. 17 (a-d) present the performance of HC and deep feature based trackers using an average precision and success over OTB2015 and TC-128 benchmarks. On OTB2015 benchmark, CSRDCF and STRCF outperformed other HC trackers in terms of precision {89.4% and 86.4%} and success {65.4% and 65.0%} shown in Fig. 17 (a). While in case of deep trackers, ECO and CCOT attained the best performance with precision {89.9% and 89.6%} and success {68.0% and 66.7%} exhibited in (Fig. 17 (b)). Likewise, over TC-128 benchmark, SRDCF and STRCF performed well using precision and

success (Fig. 17 (c)), HC trackers, while ECO and CCOT trackers maintained the highest performance (Fig. 17 (d)) among deep trackers.

E. Challenges-based Analysis

No tracker can perform best for all the tracking challenges i.e., Occlusion (OCC), Background Clutter (BC), Scale Variations (SV), Illumination Variation (IV), Deformation (DEF), Low Resolution (LR), Fast Motion (FM), Out-of-View (OV), Motion Blur (MB), In-Plane Rotation (IPR), and Out-of-Plane Rotations (OPR). Therefore, we present a challenge based evaluation of trackers and report the performance of the trackers in terms of precision (see table IV) and success (Figs. 18, 19) over OTTC.

Over the group of fast motion and motion blur videos, STRCF and SRDCF performed best among HC trackers in terms of both the precision and the success. While CCOT and ECO handled this challenge successfully among the deep trackers. Both CCOT and ECO achieved better performance for these challenges compared to all the trackers (see table IV and Figs. 18, 19). Improved accuracy of ECO and CCOT approaches is due to the fused multi-resolution feature maps computed by convolutional layers. Other trackers were not able to efficiently handle these challenges because of the fast target movement in the video.

SRDCF, CSRDCF, and STRCF handled best the occlusion and deformation challenges among HC trackers while ECO,

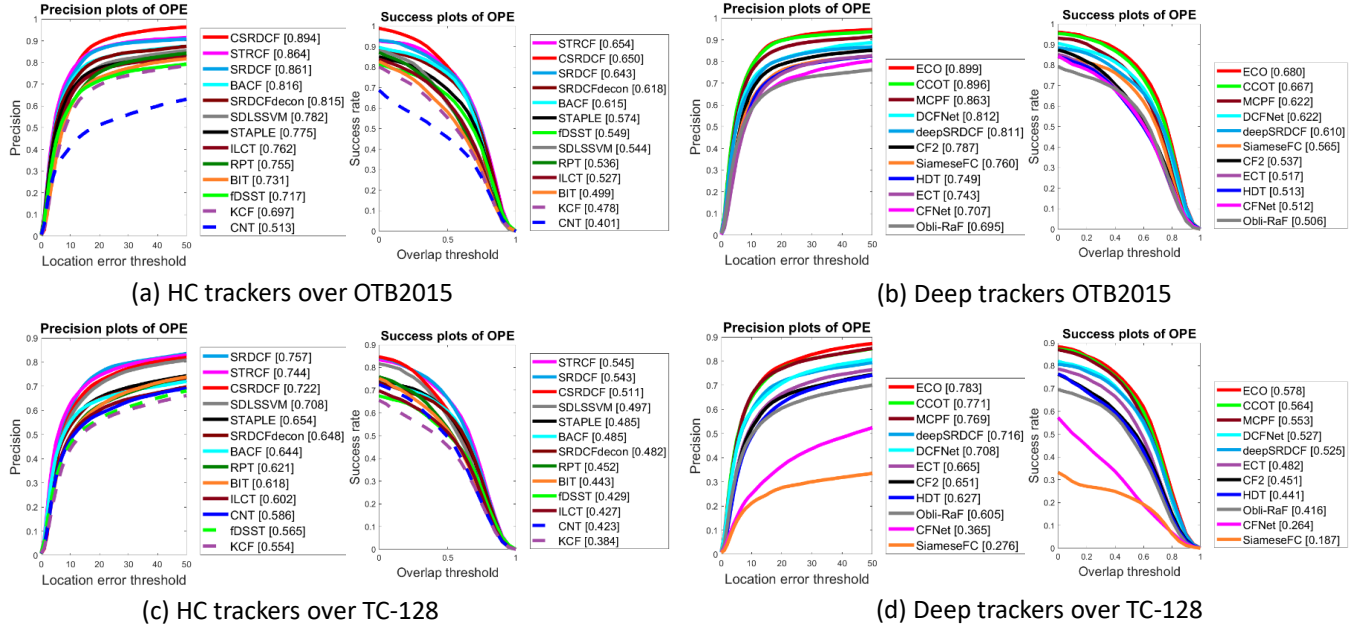


Fig. 17. Precision and success plots for handcrafted (HC) and deep features over OTB2015 and TC-128 benchmarks.

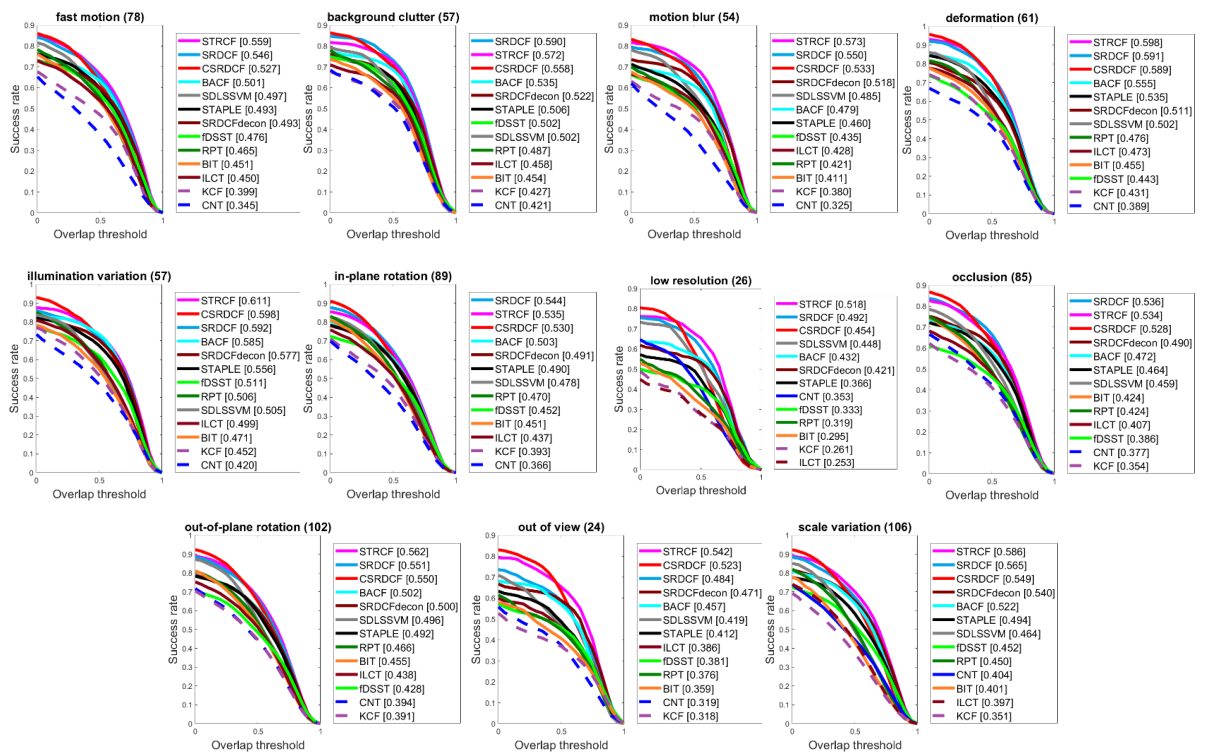


Fig. 18. Success plots of HC trackers for eleven object tracking challenges over OTTC benchmark.

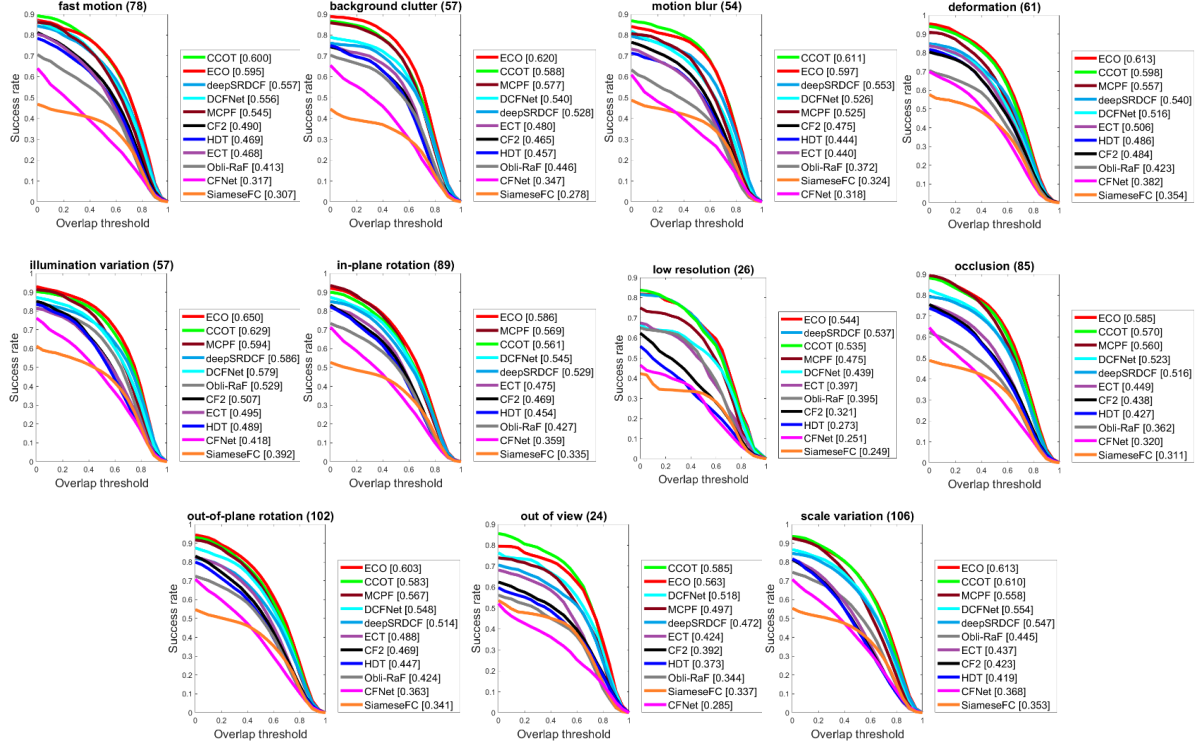


Fig. 19. Success plots of deep trackers for eleven object tracking challenges over OTTC benchmark.

TABLE IV
PRECISION FOR HC AND DEEP TRACKERS ON DIFFERENT CHALLENGES OVER OTTC BENCHMARK.

Challenges	Handcrafted Trackers													Deep Trackers												
	STRCF	SRDCF	CSRDGF	SDLSSVM	SRDGFdecon	BACF	STAPLE	IDSST	BIT	ILCT	RPT	KCF	CNT	ECO	CCOT	MCPF	deepSRDCF	DCFNet	CSRDGF	HDT	ECT	Obli-RaF	SiameseFC	CFNet		
FM	71.3	69.9	68.4	65.9	62.1	64.2	62.6	58.3	58.0	58.2	58.2	53.3	41.0	74.6	75.2	72.5	70.0	69.0	66.0	61.8	60.7	55.0	40.1	38.9		
BC	79.0	83.0	80.3	73.3	70.9	73.2	70.9	70.5	69.0	66.9	70.2	63.3	58.7	85.7	82.6	81.5	74.4	74.4	69.7	68.4	69.5	65.0	40.4	52.0		
MB	74.2	73.9	72.4	67.4	67.4	62.4	62.7	56.2	56.7	58.9	52.8	39.7	78.0	80.6	72.5	73.7	65.8	66.6	61.0	60.4	50.2	42.2	42.8			
DEF	83.7	82.2	83.0	72.2	70.0	74.9	73.6	63.5	63.5	67.4	67.9	60.5	53.7	84.2	83.6	80.1	75.1	75.1	70.7	69.7	71.6	58.4	49.1	53.2		
IPR	77.3	75.3	79.0	68.3	72.7	74.6	72.4	65.3	65.3	69.4	71.4	64.4	51.1	82.0	81.4	80.4	74.7	73.5	72.2	69.0	68.9	69.8	52.3	55.6		
DR	70.8	73.1	71.8	65.5	65.3	66.0	63.5	57.3	61.5	61.0	63.0	57.7	47.3	82.8	75.1	79.3	69.9	60.7	62.4	65.7	59.4	44.8	47.6			
LR	72.9	77.3	77.7	72.4	60.1	63.4	57.0	50.8	51.9	56.1	54.7	48.0	62.2	82.1	83.1	75.0	69.4	63.1	66.3	65.5	42.9	45.1				
OCC	70.3	71.9	71.0	65.1	63.6	60.5	60.9	49.1	57.0	56.4	56.1	49.3	49.7	77.3	74.5	77.1	68.1	67.5	61.5	59.0	51.1	41.3	42.6			
OPR	75.9	74.7	74.5	71.0	66.6	65.7	66.2	54.5	63.4	61.9	62.7	56.4	51.4	80.0	78.0	77.8	68.5	70.7	68.0	62.2	66.8	59.3	47.1	48.6		
OV	71.6	67.6	75.2	58.9	60.7	61.6	58.7	47.2	46.9	51.3	49.9	41.3	42.7	77.9	81.8	68.2	66.3	69.6	51.9	49.5	57.0	47.6	46.1	39.0		
SC	79.0	76.9	77.1	69.8	72.2	70.0	68.3	58.8	60.4	60.8	64.4	55.8	54.7	81.0	81.4	81.7	73.1	72.7	66.2	64.7	67.1	63.5	47.6	51.1		
Overall	79.1	79.6	77.6	73.2	70.8	70.9	70.4	61.7	64.8	64.8	66.6	59.9	56.7	82.0	81.1	80.3	75.4	74.0	69.3	67.2	68.7	63.0	43.5	48.1		

CCOT, and MCPF showed better performance among deep trackers for both the precision and the success measures (see table IV and Figs. 18, 19). These challenges add the background noise to the target resulting in performance degradation. The best performing tracker, ECO, solved this problem by computing Gaussian mixture component for each target.

Illumination conditions and low resolution has posed big challenge for most of the compared trackers. CSRDCF, STRCF and SRDCF handled these challenge in a more appropriate manner compared to the other HC trackers. In deep trackers, ECO, CCOT showed improved performed over both challenges. It is noted that ECO and CCOT tackled these challenges more efficiently compared to both the HC and the deep trackers because of computation of multi-resolution features from multiple convolution layers.

The influence of in-plane rotations, out of view and out-of-plane rotations presented more severe challenges for majority of the tracking algorithms. HC trackers such as CSRDCF, STRCF, SRDCF showed better performance over OV sequences using precision while STRCF showed significant im-

provement in terms of success. On the other hand, deep CCOT and ECO handled OV challenge with respect to precision and success. Over the group of IPR sequences, SRDCF, CSRDCF, and STRCF trackers exhibited leading performance among HC trackers and among deep trackers ECO, MCPF, CCOT obtained better performance. Similarly, STRCF and SRDCF tackled OPR challenge efficiently in HC category while ECO, CCOT and MCPF performed well among deep trackers. We observed that overall ECO and CCOT achieved significant efficiency over OV, IPR, and OPR challenges because of multiple convolutional operators to learn multi-resolution features. STRCF, SRDCF, and CSRDCF in HC category coped well over background clutter and scale variations and hence obtained the best precision and success as shown in Fig. 18, 19 and table IV. ECO, CCOT, and MCPF best handled these challenges in deep trackers (see Figs. 18, 19 and table IV). Overall, ECO is the best performing deep tracker in these challenges because of utilizing multiple convolutional operators and updating the GMM components.

In conclusion, it can be observed that deep trackers are more

precise, accurate, and effective as compared to HC trackers over different challenges.

F. Qualitative Evaluation

For the qualitative comparison, we selected six sequences including *Bolt*, *CarScale*, *FaceOcc1*, *Jogging-1*, *Matrix*, and *Skiing* which cover all the tracking challenges.

Figure 20 demonstrates the qualitative comparison for HC trackers. For *Bolt* sequence, most of the trackers such as CSRDCF, STRCF, and SRDCF etc tracked the player successfully while only four trackers SRDCFdecon, RPT, fDSST, and CNT were not able to track the activity of the player through out the sequence. In the *CarScale* sequence, majority of the trackers were not able to completely track the car on a road because of the scale variation. *FaceOcc1* presents the challenge of partial occlusion, where a woman rotates a book around her face. In case of *Jogging-1* sequence, occlusion because of the pole presented a major challenge for STAPLE, fDSST, KCF, RPT, ILCT and CNT trackers while the remaining trackers successfully tracked the person occluded by the pole. The lighting variations and fast motion challenges in the sequences *Matrix* and *Skiing* degraded the performance for most of the trackers excluding CSRDCF and SDLSSVM in *Skiing* and CSRDCF, fDSST and SDLSSVM in *Matrix*.

A qualitative study of deep trackers has also been performed to analyze the visual tracking performance. Obli-Raf, SiameseFC, and deepSRDCF missed the player and made their bounding box far beyond the runner for *Bolt* sequence while ECO, CCOT, HDT, CF2, CFNet, DCFNet, MCPF, and ECT turned out to be the successful trackers. For scale variation sequence *CarScale*, none of the tracker handled scaling efficiently, however, ECO, DCFNet, Obli-Raf, and SiameseFC tracked the major parts of the vehicle. Over partial occlusion *FaceOcc1* sequence, all tracker succeeded to track the face except for CFNet, although it achieved some success but eventually its performance falls off. While for complete occlusion *Jogging-1* sequence, HDT, DCFNet, and Obli-Raf presented degraded performance. Another challenging *Matrix* sequence where it is raining, HDT, DCFNet, CF2, MCPF, ECT Obli-Raf, SiameseFC, and CFNet exhibited degraded performance and only ECO, CCOT, and deepSRDCF succeeded. For challenging sequence like *Skiing*, ECO, CCOT, MCPF, SiameseFC, and DCFNet accomplished the tracking task successfully as compared to other deep trackers.

In short, qualitative study revealed CSRDCF and SRDCF as best trackers among HC tracker while ECO and CCOT showed efficient performance among deep trackers. Additionally, It is noted that these tracking algorithms employed spatial regularization using discriminative correlation filters.

G. Comparison over VOT2017

We have also reported results over VOT2017 [19] benchmark comparing the performance of various trackers. In VOT toolkit, if a tracker loses the target, it is re-initialized using the ground-truth bounding box. This procedure is named as reset property of the VOT toolbox. It should be noted that no reset

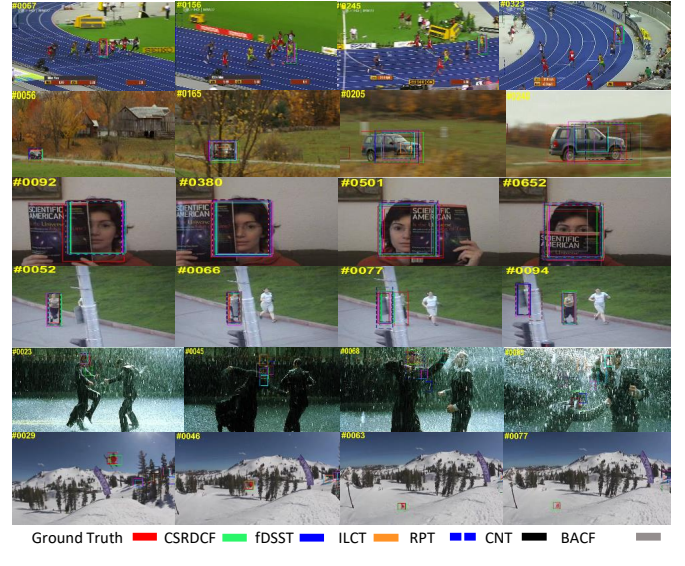


Fig. 20. Qualitative analysis of HC trackers on challenging sequences (from top to bottom *Bolt*, *CarScale*, *FaceOcc1*, *Jogging-1*, *Matrix*, and *Skiing* respectively).

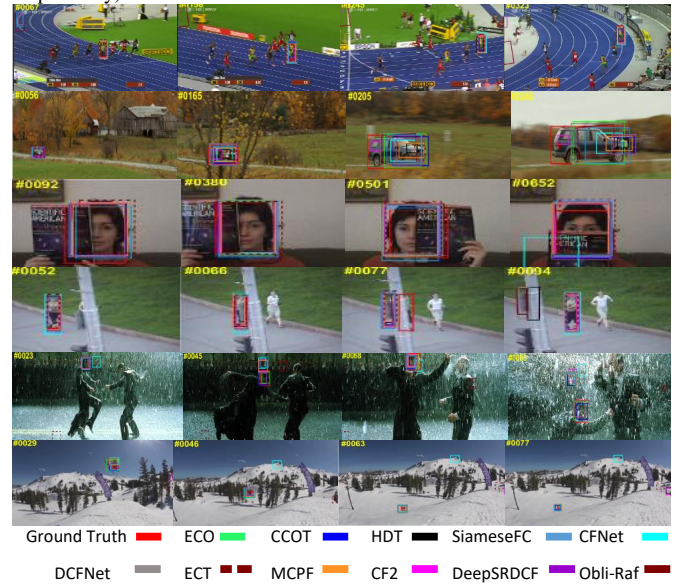


Fig. 21. Qualitative analysis of deep trackers on challenging sequences (from left to right *Bolt*, *CarScale*, *FaceOcc1*, *Jogging-1*, *Matrix*, and *Skiing* respectively).

TABLE V
COMPARISON OF HC AND DEEP TRACKERS USING ROBUSTNESS (R),
ACCURACY (A), AND EXPECTED AVERAGE OVERLAP (EO) MEASURES
FOR BASELINE AND REALTIME EXPERIMENTS OVER VOT2017.

Tracker	Baseline			Realtime			
	EO	A	R	EO	A	R	
HC trackers	CSRDCF	0.256	0.491	0.356	0.099	0.477	1.054
	STAPLE	0.169	0.530	0.688	0.170	0.530	0.688
	KCF	0.135	0.447	0.773	0.134	0.445	0.782
	SRDCF	0.119	0.490	0.974	0.058	0.377	1.999
	DSST	0.079	0.395	1.452	0.077	0.396	1.480
Deep trackers	CF2	0.286	0.509	0.281	0.059	0.339	1.723
	ECO	0.280	0.483	0.276	0.078	0.449	1.466
	CCOT	0.267	0.494	0.318	0.058	0.326	1.461
	SiameseFC	0.188	0.502	0.585	0.182	0.502	0.504
	MCPF	0.248	0.510	0.427	0.060	0.325	1.489

is performed in OTB toolkit. In addition to the reset property, VOT toolkit requires multiple runs of the same tracker on the same video to evaluate performance of that tracker, while OTB toolkit performs one pass evaluation. For performance comparison, VOT has three primary measures such as Accuracy (A), Robustness (R) and Expected Average Overlap (EAO). The average overlap score between ground truth and predicted bounding boxes for successful tracking intervals is known as accuracy. Robustness is reported as the how many times a tracker failed and required reset. Stochastic tracking algorithms are executed multiple times for each sequence. VOT toolkit reduces the potential bias added due to reset property in the accuracy measure by discarding 10 frames after re-initialization. Averaging robustness and accuracy over multiple runs for a single sequence gives the per sequence robustness and accuracy. EAO is used to measure the expected overlap score computed for typical short-term sequence lengths over an interval by averaging the scores for the expected average overlap curve (see more detail [17]). The results shown in Table V are drawn from [19]. Tracking results are shown for baseline and real-time experiments separately for handcrafted and deep feature based trackers. In VOT toolkit, in real-time experiments a tracker at the first frame, is initialized and waits for the output bounding box to be computed and the next frame to be read from memory. If the next frame becomes available before completion of computation for the previous bounding box, than that bounding box is output for the next frame as well. In baseline experiments, a bounding box is computed for each frame. In our analysis, we have included trackers with results reported in [19] and overlapping with the trackers shown in Table III. Among the compared trackers, CSRDCF performed best among HC trackers using EAO and R measures, while STAPLE performed best using A measure for the baseline experiments. On the other hand, for real-time experiments, STPALE showed significant improvement in performance among HC trackers for all measures. For deep trackers, in baseline experiments, CF2 exhibited best results with EAO=0.286, MCPF is the best with A=0.510, and ECO is the best with R=0.276. For real-time experiments, SiameseFC showed best performance in terms of all measures.

H. Speed Comparison

An efficient tracker must track target accurately and robustly with low computational cost. For real world applications, computational complexity takes a vital role in the selection of a specific tracker. Tracking model complexity and target update frequency are the fundamental reasons effecting the speed of a tracker. We have reported the average speed of the HC and deep feature based trackers over OTB2013, OTB2015, TC-128, and OTTC benchmarks (Fig. 22). For all the compared trackers, we have used default parameters as given by the original authors. For a fair speed comparison, all experiments are performed on the same computer with Intel Core i5 CPU 3.40 GHz and 8 GB RAM. GeForce GTX 650 GPU is being used for deep trackers. Overall HC trackers require less computational cost as compared to deep trackers which often take a lot of time for feature extraction

at each frame. The online model update for each frame in deep trackers incur high computational cost. The KCF tracker is ranked as the fastest tracker compared to all the trackers. Speed comparison demonstrates that KCF, fDSST and BIT HC trackers process more frames in one second than the fastest deep tracker which is SiameseFC. Some HC trackers including SRDCF, SRDCFdecon, and CNT require high computational cost therefore FPS is less than 5. Similarly, deep trackers including CCOT, MCPF, deepSRDCF, DCFNet, ECT, OblRaf, and ECT are also computational complex with speed less than 5 FPS as shown in Fig. 22.

I. Comparison of Tracking Performance over Different Features

We evaluated the performance of ECO over OTB2015 using different types of features as shown in Table VI. We compared HOG and Color Names (CN) as Hand Crafted (HC) features with deep features obtained from VGGNet and also made different feature combinations. Deep features are extracted from each layer represented as Conv i , where i is the layer index. Deep features are also extracted from more than one VGG layers, for example Conv123 are extracted from layer 1, 2 and 3. We observe that Conv12 obtained best performance compared to only HC and only deep features. However, the combination of both HOG and deep features i.e., HOG_Conv15 exhibited overall best performance. The increase in accuracy shows that there is some information in HC features which was not encoded by the deep features. Therefore, fusion of both types of features was able to obtain improved accuracy. For real-time applications, computation time is very important. In general, deep features take more execution time compared to the HC features. Thus, there is a trade-off between accuracy and computational complexity, more accurate feature combination with ECO takes more time.

J. Findings and Recommendations

In this work we have explored tracking problem using Correlation Filter based Trackers (CFTs) and Non-CFTs proposed over the past few years and we believe that it is still an open problem. We also performed an extensive analysis of state-of-the-art trackers with respect to handcrafted and deep features. Qualitative and quantitative evaluations reveal that on a broader level, CFTs have shown better performance over Non-CFTs. The CFTs are using both handcrafted and deep features. At a finer level, we observe that regularized CFTs exhibit excellent performance within this category. Therefore, we recommend the use of Regularized-CFTs because of their potential for further improvement. Spatial and temporal regularization has been used in Discriminative Correlation Filters (DCF) to improve the tracking performance.

Our study concludes that it is required to learn efficient discriminative features preserving geometric, structural, and spatial target information. Structural information encodes appearance variations while geometric information captures the shape and spatial information encodes the location of different parts. Deep convolutional features encode low-level spatial and high-level semantic information which is vital for precise

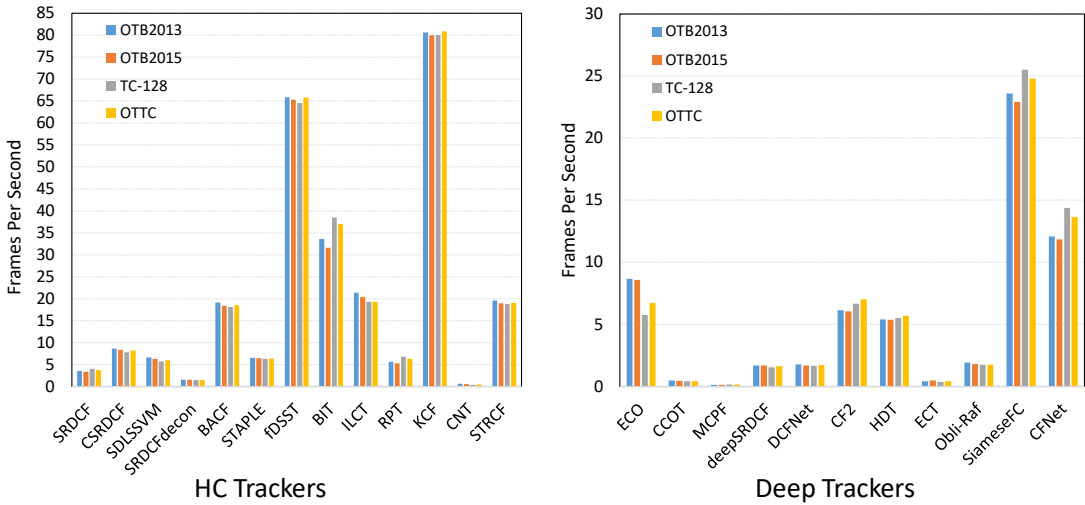


Fig. 22. Speed analysis of HC and deep trackers in frames per second.

TABLE VI
TRACKING PERFORMANCE COMPARISON OF ECO ALGORITHM USING DIFFERENT TYPES OF FEATURES

	HOG	CN	HOG_CN	Conv1	Conv2	Conv3	Conv4	Conv5	Conv12	Conv123	Conv1234	Conv12345	HOG_Conv15
Precision	78.5	58.3	80.6	69.8	77.6	62.1	69.5	73.0	81.5	74.4	73.6	73.4	90.0
Success	59.9	43.4	61.1	51.6	54.6	42.5	46.5	47.1	61.5	55.7	55.4	55.0	68.2
FPS	51.50	14.11	23.77	21.33	20.76	17.54	17.13	16.80	11.88	6.84	5.76	4.25	6.58

target positioning while HC features encode less semantic information. Thus efficient fusion of HC and deep features including low-level and high-level information captures invariant complex features from geometry and structure of targets and enhances the tracking performance.

The performance of the trackers can be improved by including temporal information along with spatial information. Recurrent Neural Network (RNN) models capture the temporal relationship among sequential images. Although trackers using RNN models are proposed to integrate temporal information including RTT [112] and SANet [127], however the improvement in results is not significant. Currently, RNN have not been much explored by the tracking community, therefore it remains unclear how much performance improvement can be obtained by employing architectures similar to RNN. Thus, it may be a possible future research direction.

Learning based tracking algorithms suffer due to lack of training data availability. Usually object bounding box is available only in the first frame. Recently, zero-shot and one-shot learning are studied to alleviate data limitation problem and it is also a new direction yet to be explored in tracking domain. In tracking-by-detection framework, online updating current frame due to limited positive samples can lead to over-fitting problem. For example, at detection stage, target is partially occluded and thus a tracker can learn noisy target shape. For long term tracking, positive target patches capturing all target shape variations are required to learn complete target appearance. Generative Adversarial Networks (GAN) [197] has ability to produce realistic images. Recently, Song et al. [198] employed GAN and proposed VITAL algorithm. Inclusion of

GAN and reinforcement learning in tracking frameworks can also effectively improve the tracking performance and is a promising future direction. In short, the tracker's ability to efficiently learn target's shape, appearance, and geometry, as well as temporal variations is vital for efficient tracking. Experimental study reveals that more accurate trackers often have high computational cost. Therefore, it is necessary to obtain high tracking speeds without losing accuracy.

V. CONCLUSION

In this study, a survey of recent visual object tracking algorithms is performed. Most of these algorithms were published during the last four years. These trackers are classified into two main groups, CFTs and Non-CFTs. Each category is further organized into different classes based on the methodology and framework. This paper provides interested readers an organized overview of the diverse tracking area as well as trends and proposed frameworks. It will help the readers to find research gaps and provides insights for developing better tracking algorithms. This study also enables the readers to select appropriate trackers for specific real world applications keeping in view the performance of the trackers over different challenges. Four different benchmarks including OTB50, OTB100, TC-128 and a new proposed benchmark OTTC are used for performance comparison of 24 algorithms using precision and success measures and execution time for each tracker. This study concludes that regularized CFTs have yielded better performance compared to the others. Spatial and temporal regularizations emphasizing the object information and suppressing the background in DCFs further enhance the tracking performance. Deep features have ability to encode

low-level and high-level information compared to handcrafted features. Efficient transfer learning while improving accuracy, robustness, and solving the limitation of training data will be new progression.

ACKNOWLEDGMENT

This study was supported by the BK21 Plus project (SW Human Resource Development Program for Supporting Smart Life) funded by the Ministry of Education, School of Computer Science and Engineering, Kyungpook National University, Korea (21A20131600005).

REFERENCES

- [1] V. A. Laurense, J. Y. Goh, and J. C. Gerdes, "Path-tracking for autonomous vehicles at the limit of friction," in *ACC*. IEEE, 2017, pp. 5586–5591.
- [2] B. Tian, Q. Yao, Y. Gu, K. Wang, and Y. Li, "Video processing techniques for traffic flow monitoring: A survey," in *ITSC*. IEEE, 2011.
- [3] A. Ali, A. Jalil, J. Niu, X. Zhao, S. Rathore, J. Ahmed, and M. A. Iftikhar, "Visual object tracking: classical and contemporary approaches," *FCS*, vol. 10, no. 1, pp. 167–188, 2016.
- [4] J. Severson, "Human-digital media interaction tracking," 2017, uS Patent 9,713,444.
- [5] S. Walker, C. Sewell, J. Park, P. Ravindran, A. Koolwal, D. Camarillo, and F. Barbagli, "Systems and methods for localizing, tracking and/or controlling medical instruments," 2017, uS Patent App. 15/466,565.
- [6] J. K. Aggarwal and L. Xia, "Human activity recognition from 3d data: A review," *PRL*, 2014.
- [7] Y. Wu, J. Lim, and M. Yang, "Online object tracking: A benchmark," in *CVPR*. IEEE, 2013, pp. 2411–2418.
- [8] ———, "Object tracking benchmark," *IEEE T-PAMI*, pp. 1834–1848, 2015.
- [9] A. Yilmaz, O. Javed, and M. Shah, "Object tracking: A survey," *ACM Comput. Surv.*, vol. 38, p. 13, 2006.
- [10] K. Cannons, "A review of visual tracking," *Dept. Comput. Sci. Eng., York Univ., Toronto, Canada, Tech. Rep. CSE-2008-07*, 2008.
- [11] A. W. Smeulders, D. M. Chu, R. Cucchiara, S. Calderara, A. Dehghan, and M. Shah, "Visual tracking: An experimental survey," *IEEE T-PAMI*, vol. 36, no. 7, pp. 1442–1468, 2014.
- [12] X. Li, W. Hu, C. Shen, Z. Zhang, A. Dick, and A. V. D. Hengel, "A survey of appearance models in visual object tracking," *ACM T-IST*, vol. 4, no. 4, p. 58, 2013.
- [13] H. Yang, L. Shao, F. Zheng, L. Wang, and Z. Song, "Recent advances and trends in visual tracking: A review," *Neurocomputing*, vol. 74, no. 18, pp. 3823–3831, 2011.
- [14] P. Li, D. Wang, L. Wang, and H. Lu, "Deep visual tracking: Review and experimental comparison," *PR*, vol. 76, pp. 323–338, 2018.
- [15] M. Kristan, R. Pflugfelder, A. Leonardis, J. Matas, F. Porikli, L. Cebovin, G. Nebehay, G. Fernandez, T. Vojir, A. Gatt *et al.*, "The visual object tracking vot2013 challenge results," in *ICCVW*. IEEE, 2013, pp. 98–111.
- [16] ———, "The visual object tracking vot2014 challenge results," pp. 191–217, 2014.
- [17] ———, "The visual object tracking vot2015 challenge results," pp. 564–586, 2015.
- [18] ———, "The visual object tracking vot2016 challenge results," 2016.
- [19] ———, "The visual object tracking vot2017 challenge results," pp. 1949–1972, 2017.
- [20] A. Graves, A. Mohamed, and G. Hinton, "Speech recognition with deep recurrent neural networks," in *ICASSP*. IEEE, 2013, pp. 6645–6649.
- [21] K. Simonyan and A. Zisserman, "Very deep convolutional networks for large-scale image recognition," *CoRR*, vol. abs/1409.1556, 2014.
- [22] K. He, X. Zhang, S. Ren, and J. Sun, "Deep residual learning for image recognition," in *CVPR*. IEEE, 2016, pp. 770–778.
- [23] B. Zhuang, L. Wang, and H. Lu, "Visual tracking via shallow and deep collaborative model," *Neurocomputing*, vol. 218, pp. 61–71, 2016.
- [24] M. Danelljan, G. Hager, F. S. Khan, and M. Felsberg, "Convolutional features for correlation filter based tracking," in *ICCVW*. IEEE, 2015.
- [25] M. Danelljan, G. Bhat, F. S. Khan, and M. Felsberg, "Eco: Efficient convolution operators for tracking," in *CVPR*. IEEE, 2017, pp. 6931–6939.
- [26] L. Bertinetto, J. Valmadre, J. F. Henriques, A. Vedaldi, and P. H. Torr, "Fully-convolutional siamese networks for object tracking," in *ECCVW*. Springer, 2016, pp. 850–865.
- [27] M. Danelljan, G. Hager, F. S. Khan, and M. Felsberg, "Learning spatially regularized correlation filters for tracking," in *ICCV*. IEEE, 2015.
- [28] A. Lukei, T. Voj, L. .n Zajc, J. Matas, and M. Kristan, "Def with channel and spatial reliability," in *CVPR*. IEEE, 2017.
- [29] T. Zhang, K. Jia, C. Xu, Y. Ma, and N. Ahuja, "Partial occlusion handling for tracking via robust part matching," in *CVPR*. IEEE, 2014.
- [30] J. Pan and B. Hu, "Robust occlusion handling in object tracking," in *CVPR*. IEEE, 2007, pp. 1–8.
- [31] A. Yilmaz, X. Li, and M. Shah, "Contour-based object tracking with occlusion handling in video acquired using mobile cameras," *IEEE T-PAMI*, vol. 26, no. 11, pp. 1531–1536, 2004.
- [32] W. Zhong, H. Lu, and M. Yang, "Robust object tracking via sparsity-based collaborative model," in *CVPR*. IEEE, 2012.
- [33] A. Adam, E. Rivlin, and I. Shimshoni, "Robust fragments-based tracking using the integral histogram," in *CVPR*. IEEE, 2006.
- [34] B. Babenko, M. Yang, and S. Belongie, "Visual tracking with online multiple instance learning," in *CVPR*. IEEE, 2009, pp. 983–990.
- [35] X. Mei and H. Ling, "Robust visual tracking using ℓ_1 minimization," in *ICCV*. IEEE, 2009, pp. 1436–1443.
- [36] Z. Kalal, J. Matas, and K. Mikolajczyk, "Pn learning: Bootstrapping binary classifiers by structural constraints," in *CVPR*. IEEE, 2010.
- [37] J. Kwon and K. M. Lee, "Visual tracking decomposition," in *CVPR*. IEEE, 2010, pp. 1269–1276.
- [38] I. Leang, S. Herbin, B. Girard, and J. Droulez, "On-line fusion of trackers for single-object tracking," *PR*, vol. 74, pp. 459–473, 2018.
- [39] J. Lee, B. K. Iwana, S. Ide, and S. Uchida, "Globally optimal object tracking with fully convolutional networks," *CoRR*, 2016.
- [40] J. Berclaz, F. Fleuret, E. Turetken, and P. Fua, "Multiple object tracking using k-shortest paths optimization," *IEEE T-PAMI*, vol. 33, no. 9, pp. 1806–1819, 2011.
- [41] L. L. Taixé, A. Milan, K. Schindler, D. Cremers, I. Reid, and S. Roth, "Tracking the trackers: An analysis of the state of the art in multiple object tracking," *CoRR*, vol. abs/1704.02781, 2017.
- [42] L. Qin, H. Snoussi, and F. Abdallah, "Object tracking using adaptive covariance descriptor and clustering-based model updating for visual surveillance," *Sensors*, 2014.
- [43] Q. Yu, T. B. Dinh, and G. Medioni, "Online tracking and reacquisition using co-trained generative and discriminative trackers," in *ECCV*. Springer, 2008, pp. 678–691.
- [44] E. Gundogdu, A. Koc, B. Solmaz, R. I. Hammoud, and A. A. Alatan, "Evaluation of feature channels for correlation-filter-based visual object tracking in infrared spectrum," in *CVPRW*. IEEE, 2016, pp. 290–298.
- [45] Y. Sui, Z. Zhang, G. Wang, Y. Tang, and L. Zhang, "Real-time visual tracking: Promoting the robustness of correlation filter learning," in *ECCV*. Springer, 2016.
- [46] K. Chen, W. Tao, and S. Han, "Visual object tracking via enhanced structural correlation filter," *Elsevier Inf. Sci.*, vol. 394, pp. 232–245, 2017.
- [47] S. Gu, Y. Zheng, and C. Tomasi, "Efficient visual object tracking with online nearest neighbor classifier," in *ACCV*. Springer, 2010.
- [48] Z. H. Khan, I. Y.-H. Gu, and A. G. Backhouse, "Robust visual object tracking using multi-mode anisotropic mean shift and particle filters," *IEEE T-CSVT*, vol. 21, no. 1, pp. 74–87, 2011.
- [49] H. Gong, J. Sim, M. Likhachev, and J. Shi, "Multi-hypothesis motion planning for visual object tracking," in *ICCV*. IEEE, 2011, pp. 619–626.
- [50] Q. Liu, X. Zhao, and Z. Hou, "Survey of single-target visual tracking methods based on online learning," *IET-CV*, 2014.
- [51] S. Zhang, H. Yao, X. Sun, and X. Lu, "Sparse coding based visual tracking: Review and experimental comparison," *PR*, 2013.
- [52] M. Yang, Y. Wu, and G. Hua, "Context-aware visual tracking," *IEEE T-PAMI*, vol. 31, no. 7, pp. 1195–1209, 2009.
- [53] M. Yang, Y. Wu, and S. Lao, "Intelligent collaborative tracking by mining auxiliary objects," in *CVPR*, vol. 1. IEEE, 2006, pp. 697–704.
- [54] Z. Chen, Z. Hong, and D. Tao, "An experimental survey on correlation filter-based tracking," *CoRR*, vol. abs/1509.05520, 2015.
- [55] M. S. Arulampalam, S. Maskell, N. Gordon, and T. Clapp, "A tutorial on particle filters for online nonlinear/non-gaussian bayesian tracking," *IEEE T-SP*, vol. 50, no. 2, pp. 174–188, 2002.
- [56] P. F. Felzenszwalb, R. B. Girshick, D. McAllester, and D. Ramanan, "Object detection with discriminatively trained part-based models," *IEEE T-PAMI*, vol. 32, no. 9, pp. 1627–1645, 2010.

[57] L. Essannouni, E. Ibn-Elhaj, and D. Aboutajdine, "Fast cross-spectral image registration using new robust correlation," *Springer JRTIP*, vol. 1, no. 2, pp. 123–129, 2006.

[58] M. Savvides, B. V. Kumar, and P. Khosla, "Face verification using correlation filters," *AutoID*, pp. 56–61, 2002.

[59] M. D. Rodriguez, J. Ahmed, and M. Shah, "Action mach a spatio-temporal maximum average correlation height filter for action recognition," in *CVPR*. IEEE, 2008, pp. 1–8.

[60] D. S. Bolme, J. R. Beveridge, B. A. Draper, and Y. M. Lui, "Visual object tracking using adaptive correlation filters," in *CVPR*. IEEE, 2010.

[61] D. S. Bolme, B. A. Draper, and J. R. Beveridge, "Average of synthetic exact filters," in *CVPR*. IEEE, 2009, pp. 2105–2112.

[62] J. F. Henriques, R. Caseiro, P. Martins, and J. Batista, "Exploiting the circulant structure of tracking-by-detection with kernels," in *ECCV*. Springer, 2012, pp. 702–715.

[63] ——, "High-speed tracking with kernelized correlation filters," *IEEE T-PAMI*, vol. 37, no. 3, pp. 583–596, 2015.

[64] M. Danelljan, F. S. Khan, M. Felsberg, and J. V. de Weijer, "Adaptive color attributes for real-time visual tracking," in *CVPR*. IEEE, 2014.

[65] R. J. Williams and D. Zipser, "A learning algorithm for continually running fully recurrent neural networks," *MIT Press NC*, vol. 1, no. 2, pp. 270–280, 1989.

[66] C. Ma, J. B. Huang, X. Yang, and M. Yang, "Hierarchical convolutional features for visual tracking," in *ICCV*. IEEE, 2015, pp. 3074–3082.

[67] C. Ma, J. Huang, X. Yang, and M. Yang, "Robust visual tracking via hierarchical convolutional features," *IEEE T-PAMI*, 2018.

[68] Y. Qi, S. Zhang, L. Qin, H. Yao, Q. Huang, J. Lim, and M. Yang, "Hedged deep tracking," in *CVPR*. IEEE, 2016, pp. 4303–4311.

[69] C. Ma, X. Yang, C. Zhang, and M. Yang, "Long-term correlation tracking," in *CVPR*. IEEE, 2015, pp. 5388–5396.

[70] C. Ma, J.-B. Huang, X. Yang, and M.-H. Yang, "Adaptive correlation filters with long-term and short-term memory for object tracking," *IJCV*, pp. 1–26, 2018.

[71] T. Zhang, C. Xu, and M. Yang, "Multi-task correlation particle filter for robust object tracking," in *CVPR*. IEEE, July 2017, pp. 4819–4827.

[72] M. Danelljan, G. Häger, F. S. Khan, and M. Felsberg, "Discriminative scale space tracking," *IEEE T-PAMI*, vol. 39, pp. 1561–1575, 2017.

[73] L. Bertinetto, J. Valmadre, S. Golodetz, O. Miksik, and P. Torr, "Staple complementary learners for realtime tracking," in *CVPR*. IEEE, 2016.

[74] M. Zhang, J. Xing, J. Gao, X. Shi, Q. Wang, and W. Hu, "Joint scale-spatial correlation tracking with adaptive rotation estimation," in *ICCVW*. IEEE, 2015, pp. 32–40.

[75] M. Zhang, J. Xing, J. Gao, and W. Hu, "Robust visual tracking using joint scale-spatial correlation filters," in *ICIP*. IEEE, 2015, pp. 1468–1472.

[76] Y. Song, C. Ma, L. Gong, J. Zhang, R. Lau, and M. Yang, "Crest convolutional residual learning for tracking," in *ICCV*. IEEE, 2017.

[77] H. Fan and H. Ling, "Parallel tracking and verifying: A framework for real-time and high accuracy visual tracking," 2017.

[78] L. Wang, W. Ouyang, X. Wang, and H. Lu, "Stct: Sequentially training convolutional networks for visual tracking," in *CVPR*. IEEE, 2016.

[79] Z. Hong, Z. Chen, C. Wang, X. Mei, D. Prokhorov, and D. Tao, "Multi-store tracker (muster): A cognitive psychology inspired approach to object tracking," in *CVPR*. IEEE, 2015, pp. 749–758.

[80] Z. Chi, H. Li, H. Lu, and M. Yang, "Dual deep network for visual tracking," *IEEE T-IP*, vol. 26, no. 4, pp. 2005–2015, 2017.

[81] M. Wang, Y. Liu, and Z. Huang, "Large margin object tracking with circulant feature maps," pp. 4800–4808, 2017.

[82] M. Ozuysal, P. Fua, and V. Lepetit, "Fast keypoint recognition in ten lines of code," in *CVPR*. IEEE, 2007, pp. 1–8.

[83] M. Danelljan, G. Häger, F. S. Khan, and M. Felsberg, "Adaptive decontamination of the training set: A unified formulation for discriminative visual tracking," in *CVPR*. IEEE, 2016, pp. 1430–1438.

[84] F. Li, C. Tian, W. Zuo, L. Zhang, and M. Yang, "Learning spatial-temporal regularized correlation filters tracking," in *CVPR*. IEEE, 2018.

[85] S. Gladh, M. Danelljan, F. S. Khan, and M. Felsberg, "Deep motion features for visual tracking," in *ICPR*. IEEE, 2016, pp. 1243–1248.

[86] M. Danelljan, A. Robinson, F. S. Khan, and M. Felsberg, "Beyond correlation filters: Learning continuous convolution operators for visual tracking," in *ECCV*. Springer, 2016.

[87] M. Mueller, N. Smith, and B. Ghanem, "Context-aware correlation filter tracking," pp. 1387–1395, 2017.

[88] H. K. Galoogahi, A. Fagg, and S. Lucey, "Learning background-aware correlation filters for visual tracking," in *ICCV*. IEEE, 2017.

[89] J. Choi, H. Jin Chang, J. Jeong, Y. Demiris, and J. Young Choi, "Visual tracking using attention-modulated disintegration and integration," in *CVPR*. IEEE, 2016, pp. 4321–4330.

[90] J. Choi, H. Chang, S. Yun, T. Fischer, Y. Demiris, and J. Choi, "Attentional correlation filter network for adaptive visual tracking," in *CVPR*. IEEE, 2017, pp. 4828–4837.

[91] H. Hu, B. Ma, J. Shen, and L. Shao, "Manifold regularized correlation object tracking," *IEEE T-NNLS*, 2017.

[92] H. K. Galoogahi, T. Sim, and S. Lucey, "Correlation filters with limited boundaries," in *CVPR*. IEEE, 2015, pp. 4630–4638.

[93] G. Chéron, I. Laptev, and C. Schmid, "P-cnn: Pose-based cnn features for action recognition," in *ICCV*. IEEE, 2015, pp. 3218–3226.

[94] Y. Li and J. Zhu, "A scale adaptive kernel correlation filter tracker with feature integration," in *ECCVW*. Springer, 2014, pp. 254–265.

[95] J. Choi and J. Y. Choi, "User interactive segmentation with partially growing random forest," in *ICIP*. IEEE, 2015.

[96] L. L. Taixé, C. C. Ferrer, and K. Schindler, "Learning by tracking: Siamese cnn for robust target association," in *CVPRW*. IEEE, 2016, pp. 33–40.

[97] F. Schroff, D. Kalenichenko, and J. Philbin, "Facenet: A unified embedding for face recognition and clustering," in *CVPR*. IEEE, 2015.

[98] J. Zbontar and Y. LeCun, "Computing the stereo matching cost with a convolutional neural network," in *CVPR*. IEEE, 2015, pp. 1592–1599.

[99] A. Dosovitskiy, P. Fischer, E. Ilg, P. Hausser, C. Hazirbas, V. Golkov, P. v. d. Smagt, D. Cremers, and T. Brox, "Flownet: Learning optical flow with convolutional networks," in *ICCV*. IEEE, 2015, pp. 2758–2766.

[100] A. Karpathy, G. Toderici, S. Shetty, T. Leung, R. Sukthankar, and L. F. Fei, "Large-scale video classification with convolutional neural networks," in *CVPR*. IEEE, 2014, pp. 1725–1732.

[101] S. Zagoruyko and N. Komodakis, "Learning to compare image patches via convolutional neural networks," in *CVPR*. IEEE, 2015.

[102] S. Chopra, R. Hadsell, and Y. LeCun, "Learning similarity metric discriminatively, with application face verification," in *CVPR*. IEEE, 2005.

[103] Q. Guo, W. Feng, C. Zhou, R. Huang, L. Wan, and S. Wang, "Learning dynamic siamese network for visual tracking," in *ICCV*. IEEE, 2017.

[104] J. Valmadre, L. Bertinetto, J. F. Henriques, A. Vedaldi, and P. H. Torr, "End-to-end representation learning for correlation filter based tracking," *CVPR*, pp. 5000–5008, 2017.

[105] Q. Wang, J. Gao, J. Xing, M. Zhang, and H. W., "Dcfnet: Discriminant correlation filters network for visual tracking," *CoRR*, vol. abs/1704.04057, 2017.

[106] C. Huang, S. Lucey, and D. Ramanan, "Learning policies for adaptive tracking with deep feature cascades," in *ICCV*. IEEE, 2017.

[107] D. Forsyth, "Object detection with discriminatively trained part-based models," *Computer*, vol. 47, no. 2, pp. 6–7, 2014.

[108] A. Prioletti, A. Møgelmose, P. Grisleri, M. M. Trivedi, A. Broggi, and T. B. Moeslund, "Part-based pedestrian detection and feature-based tracking for driver assistance: real-time, robust algorithms, and evaluation," *IEEE T-ITS*, vol. 14, no. 3, pp. 1346–1359, 2013.

[109] P. Karczmarek, A. Kierszty, W. Pedrycz, and M. Dolecki, "An application of chain code-based local descriptor and its extension to face recognition," *PR*, vol. 65, pp. 26–34, 2017.

[110] T. Liu, G. Wang, and Q. Yang, "Real-time part-based visual tracking via adaptive correlation filters," in *CVPR*. IEEE, 2015, pp. 4902–4912.

[111] Y. Li, J. Zhu, and S. C. Hoi, "Reliable patch trackers: Robust visual tracking by exploiting reliable patches," in *CVPR*. IEEE, 2015, pp. 353–361.

[112] Z. Cui, S. Xiao, J. Feng, and S. Yan, "Recurrently target-attending tracking," in *CVPR*. IEEE, 2016, pp. 1449–1458.

[113] S. Liu, T. Zhang, X. Cao, and C. Xu, "Structural correlation filter for robust visual tracking," in *CVPR*. IEEE, 2016, pp. 4312–4320.

[114] W. Chen, K. Zhang, and Q. Liu, "Robust visual tracking via patch based kernel correlation filters with adaptive multiple feature ensemble," *Neurocomputing*, vol. 214, pp. 607–617, 2016.

[115] A. Lukežič, L. Zajc, and M. Kristan, "Deformable parts correlation filters for robust visual tracking," *IEEE T-C*, vol. 48, no. 6, pp. 1849–1861, 2018.

[116] R. Blum and Z. Liu, "Multi-sensor image fusion and its applications special series on sig. proc. and comm." 2006.

[117] X. Chen, P. Flynn, and K. Bowyer, "Fusion of infrared and range data: Multi-modal face images," in *ICB*. Springer, 2006, pp. 55–63.

[118] F. Wang, Y. Wu, P. Zhang, Q. Zhang, and M. Li, "Unsupervised sar image segmentation using ambiguity label information fusion in triplet

markov fields model," *IEEE Geoscience and Remote Sensing Letters*, vol. 14, no. 9, pp. 1479–1483, 2017.

[119] M. Farid, A. Mahmood, and S. AlMaadeed, "Multi-focus image fusion using content adaptive blurring," *Inf Fusion*, vol. 45, pp. 96–112, 2019.

[120] C. Luo, B. Sun, Q. Deng, Z. Wang, and D. Wang, "Comparison of different level fusion schemes for infrared-visible object tracking: An experimental survey," in *ICRAS*. IEEE, 2018, pp. 1–5.

[121] G. Wang, J. Wang, W. Tang, and N. Yu, "Robust visual tracking with deep feature fusion," in *ICASSP*. IEEE, 2017, pp. 1917–1921.

[122] M. K. Rapuru, S. Kakanuru, P. M. Venugopal, D. Mishra, and G. Subrahmanyam, "Correlation-based tracker-level fusion for robust visual tracking," *IEEE T-IP*, vol. 26, no. 10, pp. 4832–4842, 2017.

[123] L. Ma, J. Lu, J. Feng, and J. Zhou, "Multiple feature fusion via weighted entropy for visual tracking," in *ICCV*, 2015, pp. 3128–3136.

[124] B. Bai, B. Zhong, G. Ouyang, P. Wang, X. Liu, Z. Chen, and C. Wang, "Kernel correlation filters for visual tracking with adaptive fusion of heterogeneous cues," *Neurocomputing*, vol. 286, pp. 109–120, 2018.

[125] Z. Kalal, K. Mikolajczyk, J. Matas *et al.*, "Tracking-learning-detection," *IEEE T-PAMI*, vol. 34, no. 7, p. 1409, 2012.

[126] H. Nam and B. Han, "Learning multi-domain convolutional neural networks for visual tracking," in *CVPR*. IEEE, 2016, pp. 4293–4302.

[127] H. Fan and H. Ling, "Sanet: Structure-aware network for visual tracking," *CVPRW*, pp. 2217–2224, 2017.

[128] B. Han, J. Sim, and H. Adam, "Branchout: regularization for online ensemble tracking with cnn," in *CVPR*. IEEE, 2017, pp. 521–530.

[129] K. Zhang, Q. Liu, Y. Wu, and M. Yang, "Robust visual tracking via convolutional networks without training," *IEEE TIP*, vol. 25, no. 4, pp. 1779–1792, 2016.

[130] C. Gao, F. Chen, J. Yu, R. Huang, and N. Sang, "Robust tracking using exemplar-based detectors," *IEEE T-CSVT*, vol. 27, no. 2, pp. 300–312, 2017.

[131] C. Gao, H. Shi, J. Yu, and N. Sang, "Enhancement of elda based on cnn and adaptive model update," *Sensors*, vol. 16, no. 4, p. 545, 2016.

[132] B. Cai, X. Xu, X. Xing, K. Jia, J. Miao, and D. Tao, "Bit: Biologically inspired tracker," *IEEE T-IP*, vol. 25, no. 3, pp. 1327–1339, 2016.

[133] S. Yun, J. Choi, Y. Yoo, K. Yun, and J. Choi, "Action-decision net. for tracking with deep reinforcement learning," in *CVPR*. IEEE, 2017.

[134] D. Zhang, H. Maei, X. Wang, and Y.-F. Wang, "Deep reinforcement learning for visual object tracking in videos," *CoRR*, vol. abs/1701.08936, 2017.

[135] L. Zhang, J. Varadarajan, P. Suganthan, N. Ahuja, and P. Moulin, "Robust tracking using oblique random forests," in *CVPR*. IEEE, 2017.

[136] Z. Teng, J. Xing, Q. Wang, C. Lang, S. Feng, and Y. Jin, "Robust object tracking based on temporal and spatial deep networks," in *ICCV*. IEEE, 2017, pp. 1153–1162.

[137] J. Ning, J. Yang, S. Jiang, L. Zhang, and M. Yang, "Object tracking via dual linear structured svm and explicit feature map," in *CVPR*. IEEE, 2016, pp. 4266–4274.

[138] J. Gao, T. Zhang, X. Yang, and C. Xu, "Deep relative tracking," *IEEE T-IP*, vol. 26, no. 4, pp. 1845–1858, 2017.

[139] H. Li, Y. Li, and F. Porikli, "Deeptrack: Learning discriminative feature representations online for robust visual tracking," *IEEE T-IP*, vol. 25, no. 4, pp. 1834–1848, 2016.

[140] R. Girshick, J. Donahue, T. Darrell, and J. Malik, "Rich feature hierarchies for accurate object detection and semantic segmentation," in *CVPR*. IEEE, 2014, pp. 580–587.

[141] S. Hare, A. Saffari, and P. H. Torr, "Struck: Structured output tracking with kernels," in *ICCV*, 2011.

[142] D. Ramanan, "Dual coordinate solvers for large-scale structural svms," *arXiv preprint arXiv:1312.1743*, 2013.

[143] D. Held, S. Thrun, and S. Savarese, "Learning to track at 100 fps with deep regression networks," in *ECCV*. Springer, 2016, pp. 749–765.

[144] C. Zhang, J. C. Platt, and P. A. Viola, "Multiple instance boosting for object detection," in *Adv NIPS*, 2006, pp. 1417–1424.

[145] M. Guillaumin, J. J. Verbeek, and C. Schmid, "Multiple instance metric learning from automatically labeled bags of faces," in *ECCV*. Springer, 2010, pp. 634–647.

[146] S. Ali and M. Shah, "Human action recognition in videos using kinematic features and multiple instance learning," *IEEE T-PAMI*, vol. 32, no. 2, pp. 288–303, 2010.

[147] B. Babenko, M. Yang, and S. Belongie, "Robust object tracking with online multiple instance learning," *IEEE T-PAMI*, vol. 33, no. 8, pp. 1619–1632, 2011.

[148] Z. Wang, L. Wang, and H. Zhang, "Patch based multiple instance learning algorithm for object tracking," *Comp. Int. and Neurosc.*, 2017.

[149] H. Yang, S. Qu, and Z. Zheng, "Visual tracking via online discriminative multiple instance metric learning," *Springer MTA*, pp. 1–19, 2017.

[150] V. Sharma and K. Mahapatra, "Mil based visual tracking with kernel and scale adaptation," *Sig. Pro.: Img. Comm.*, vol. 53, pp. 51–64, 2017.

[151] C. Xu, W. Tao, Z. Meng, and Z. Feng, "Robust visual tracking via online multiple instance learning with fisher information," *Elsevier PR*, vol. 48, no. 12, pp. 3917–3926, 2015.

[152] M. Abdechiri, K. Faez, and H. Amindavar, "Visual object tracking with online weighted chaotic multiple instance learning," *Neurocomputing*, vol. 247, pp. 16–30, 2017.

[153] R. Tao, E. Gavves, and A. W. Smeulders, "Siamese instance search for tracking," in *CVPR*. IEEE, 2016, pp. 1420–1429.

[154] X. Wang, C. Li, B. Luo, and J. Tang, "Sint++: Robust visual tracking via adversarial positive instance generation," in *CVPR*. IEEE, 2018.

[155] K. Chen and W. Tao, "Once for all: a two-flow convolutional neural network for visual tracking," *IEEE T-CSVT*, 2017.

[156] J. Choi, J. Kwon, and K. Lee, "Visual tracking by reinforced decision making," *arXiv preprint arXiv:1702.06291*, 2017.

[157] A. Li and S. Yan, "Object tracking with only background cues," *IEEE T-CSVT*, vol. 24, no. 11, pp. 1911–1919, 2014.

[158] R. Achanta, A. Shaji, K. Smith, A. Lucchi, P. Fua, and S. Süsstrunk, "Slic superpixels compared to state-of-the-art superpixel methods," *IEEE T-PAMI*, vol. 34, no. 11, pp. 2274–2282, 2012.

[159] Y. Z. Brekha Brekha, Arif Mahmood and C. Zhang, "Robustness analysis of superpixel algorithms to image blur, additive gaussian noise, and impulse noise," *SPIE EI*, vol. 26, p. 61604, 2017.

[160] G. Mori, X. Ren, A. Efros, and J. Malik, "Recovering human body config. combining segmentation and recog." in *CVPR*. IEEE, 2004.

[161] J. Wu, A. Osuntogun, T. Choudhury, M. Philipose, and J. M. Rehg, "A scalable approach to activity recognition based on object use," in *ICCV*. IEEE, 2007, pp. 1–8.

[162] W. Huang, R. Hu, C. Liang, W. Ruan, and B. Luo, "Structural superpixel descriptor for visual tracking," in *IJCNN*. IEEE, 2017, pp. 3146–3152.

[163] L. Wang, H. Lu, and M. Yang, "Constrained superpixel tracking," *IEEE T-C*, pp. 1030–1041, 2018.

[164] J. Wang, W. Liu, W. Xing, and S. Zhang, "Two-level superpixel and feedback based visual object tracking," *Neurocomputing*, vol. 267, pp. 581–596, 2017.

[165] F. Yang, H. Lu, and M. Yang, "Robust superpixel tracking," *IEEE T-IP*, vol. 23, no. 4, pp. 1639–1651, 2014.

[166] H. Nam, M. Baek, and B. Han, "Modeling and propagating cnns in a tree structure for visual tracking," *CoRR*, vol. abs/1608.07242, 2016.

[167] B. Zhang, Z. Li, A. Perina, A. Del Bue, V. Murino, and J. Liu, "Adaptive local movement modeling for robust object tracking," *IEEE T-CSVT*, vol. 27, no. 7, pp. 1515–1526, 2017.

[168] I. Filali, M. S. Alilli, and N. Benblidia, "Multi-scale salient object detection using graph ranking and global-local saliency refinement," *Elsevier Signal Process Image*, vol. 47, pp. 380–401, 2016.

[169] M. Li and H. Leung, "Multiview skeletal interaction recognition using active joint interaction graph," *IEEE T-M*, vol. 18, no. 11, pp. 2293–2302, 2016.

[170] H. Meena, K. Sharma, and S. Joshi, "Improved facial expression recognition using graph sig. pro." *IET EL*, vol. 53, no. 11, pp. 718–720, 2017.

[171] T. Wang and H. Ling, "Gracker: A graph-based planar object tracker," *T-PAMI*, vol. 40, no. 6, pp. 1494–1501, 2018.

[172] D. Du, H. Qi, W. Li, L. Wen, Q. Huang, and S. Lyu, "Online deformable object tracking based on structure-aware hyper-graph," *T-IP*, vol. 25, no. 8, pp. 3572–3584, 2016.

[173] D. Du, H. Qi, L. Wen, Q. Tian, Q. Huang, and S. Lyu, "Geometric hypergraph learning for visual tracking," *IEEE T-C*, vol. 47, no. 12, pp. 4182–4195, 2017.

[174] D. Yeo, J. Son, B. Han, and J. H Han, "Superpixel-based tracking-by-segmentation using markov chains," in *CVPR*. IEEE, 2017, pp. 511–520.

[175] W. Ouyang, X. Zeng, X. Wang, S. Qiu, P. Luo, Y. Tian, H. Li, S. Yang, Z. Wang, H. Li, K. Wang, J. Yan, C. C. Loy, and X. Tang, "Deepid-net: Object detection with deformable part based convolutional neural networks," *IEEE T-PAMI*, vol. 39, no. 7, pp. 1320–1334, 2017.

[176] Y. Du, Y. Fu, and L. Wang, "Representation learning of temporal dynamics for skeleton-based action recognition," *IEEE T-IP*, vol. 25, no. 7, pp. 3010–3022, 2016.

[177] J. Zhang, Y. Deng, Z. Guo, and Y. Chen, "Face recognition using part-based dense sampling local features," *Neurocomputing*, vol. 184, pp. 176–187, 2016.

- [178] R. Yao, Q. Shi, C. Shen, Y. Zhang, and A. van den Hengel, "Part-based robust tracking using online latent structured learning," *IEEE T-CSVT*, vol. 27, no. 6, pp. 1235–1248, 2017.
- [179] J. Wang, C. Fei, L. Zhuang, and N. Yu, "Part-based multi-graph ranking for visual tracking," in *ICIP*. IEEE, 2016.
- [180] F. Li, X. Jia, C. Xiang, and H. Lu, "Visual tracking with structured patch-based model," *IVC*, vol. 60, pp. 124–133, 2017.
- [181] J. Gao, T. Zhang, X. Yang, and C. Xu, "P2t: Part-to-target tracking via deep regression learning," *IEEE TIP*, vol. 27, no. 6, pp. 3074–3086, 2018.
- [182] S. Hare, S. Golodetz, A. Saffari, V. Vineet, M. M. Cheng, S. L. Hicks, and P. H. Torr, "Struck: Structured output tracking with kernels," *IEEE T-PAMI*, vol. 38, pp. 2096–2109, 2016.
- [183] S. Lou, X. Zhao, Y. Chuang, H. Yu, and S. Zhang, "Graph regularized sparsity discriminant analysis for face recognition," *Neurocomputing*, vol. 173, pp. 290–297, 2016.
- [184] H. Peng, B. Li, H. Ling, W. Hu, W. Xiong, and S. J. Maybank, "Salient object detection via structured matrix decomposition," *IEEE T-PAMI*, vol. 39, no. 4, pp. 818–832, 2017.
- [185] A. Romero, C. Gatta, and G. Camps-Valls, "Unsupervised deep feature extraction for remote sensing image classification," *IEEE T-GRS*, vol. 54, no. 3, pp. 1349–1362, 2016.
- [186] T. Zhang, S. Liu, C. Xu, S. Yan, B. Ghanem, N. Ahuja, and M. Yang, "Structural sparse tracking," in *CVPR*. IEEE, 2015, pp. 150–158.
- [187] T. Zhang, C. Xu, and M.-H. Yang, "Robust structural sparse tracking," *IEEE T-PAMI*, 2018.
- [188] J. Guo, T. Xu, Z. Shen, and G. Shi, "Visual tracking via sparse representation with reliable structure constraint," *IEEE SPL*, vol. 24, no. 2, pp. 146–150, 2017.
- [189] Y. Yi, Y. Cheng, and C. Xu, "Visual tracking based on hierarchical framework and sparse representation," *Springer MTA*, pp. 1–23, 2017.
- [190] T. Zhang, B. Ghanem, S. Liu, C. Xu, and N. Ahuja, "Robust tracking via exclusive context modeling," *IEEE T-C*, vol. 46, no. 1, pp. 51–63, 2016.
- [191] T. Zhang, S. Liu, N. Ahuja, M. Yang, and B. Ghanem, "Robust tracking via consistent low-rank sparse learning," *IJCV*, 2015.
- [192] H. Li, C. Shen, and Q. Shi, "Real-time visual tracking using compressive sensing," in *CVPR*. IEEE, 2011, pp. 1305–1312.
- [193] X. Jia, H. Lu, and M. Yang, "Visual tracking via adaptive structural local sparse appearance model," in *CVPR*. IEEE, 2012, pp. 1822–1829.
- [194] T. Zhang, B. Ghanem, S. Liu, and N. Ahuja, "Robust visual tracking via multi-task sparse learning," in *CVPR*. IEEE, 2012, pp. 2042–2049.
- [195] P. Liang, E. Blasch, and H. Ling, "Encoding color information for visual tracking: Algorithms and benchmark," *IEEE T-IP*, vol. 24, no. 12, pp. 5630–5644, 2015.
- [196] A. Vedaldi and K. Lenc, "Matconvnet: Convolutional neural networks for matlab," in *ACMMM*. ACM, 2015.
- [197] I. Goodfellow, J. P. Abadie, M. Mirza, B. Xu, D. W. Farley, S. Ozair, A. Courville, and Y. Bengio, "Generative adversarial nets," in *NIPS*, 2014.
- [198] Y. Song, C. Ma, X. Wu, L. Gong, L. Bao, W. Zuo, C. Shen, L. Rynson, and M.-H. Yang, "Vital: Visual tracking via adversarial learning," in *CVPR*. IEEE, 2018.